

Calcium Inactivation of Calcium Release in Frog Cut Muscle Fibers That Contain Millimolar EGTA or Fura-2

DE-SHIEN JONG, PAUL C. PAPE, S. M. BAYLOR,*
and W. KNOX CHANDLER

From the Department of Cellular and Molecular Physiology, Yale University School of Medicine, New Haven, Connecticut 06510-8026; and *Department of Physiology, University of Pennsylvania School of Medicine, Philadelphia, Pennsylvania 19104-6085

ABSTRACT Cut muscle fibers from *Rana temporaria* (sarcomere length, 3.4–4.2 μm) were mounted in a double Vaseline-gap chamber (14–15°C) and equilibrated with end-pool solutions that contained 20 mM EGTA and 1.76 mM Ca. Sarcoplasmic reticulum (SR) Ca release was estimated from changes in pH (Pape, P. C., D.-S. Jong, and W. K. Chandler. 1995. *Journal of General Physiology*. 106:000–000). Although the amplitude and duration of the [Ca] transient, as well as its spatial spread from the release sites, are reduced by EGTA, SR Ca release elicited by either depolarizing voltage-clamp pulses or action potentials behaved in a manner consistent with Ca inactivation of Ca release. After a step depolarization to –20 or 10 mV, the rate of SR Ca release, corrected for SR Ca depletion, reached a peak value within 5–15 ms and then rapidly decreased to a quasi-steady level that was about half the peak value; the time constant of the last half of the decrease was usually 2–4 ms. Immediately after an action potential or a 10–15 ms prepulse to –20 mV, the peak rate of SR Ca release elicited by a second stimulation, as well as the fractional amount of release, were substantially decreased. The rising phase of the rate of release was also reduced, suggesting that at least 0.9 of the ability of the SR to release Ca had been inactivated by the first stimulation. There was little change in intramembranous charge movement, suggesting that the changes in SR Ca release were not caused by changes in its voltage activation. These effects of a first stimulation on the rate of SR Ca release elicited by a second stimulation recovered during repolarization to –90 mV; the time constant of recovery was ~25 ms in the action-potential experiments and ~50 ms in the voltage-clamp experiments. Fura-2, which is able to bind Ca more rapidly than EGTA and hence reduce the amplitude of the [Ca] transient and its spatial spread from release sites by a greater amount, did not prevent Ca inactivation of Ca release, even at con-

Address correspondence to: Dr. W. K. Chandler, Department of Cellular and Molecular Physiology, Yale University School of Medicine, 333 Cedar Street, New Haven, CT 06510-8026.

Dr. Jong's current address is Department of Animal Science, National Taiwan University, Taipei, Taiwan, R.O.C.

Dr. Pape's current address is Département de Physiologie et Biophysique, Faculté de Médecine, Université de Sherbrooke, Sherbrooke, Québec, Canada J1H5N4.

centrations as large as 6–8 mM. These effects of Ca inactivation of Ca release can be simulated by the three-state, two-step model proposed by Schneider, M. F., and B. J. Simon (1988. *Journal of Physiology*. 405:727–745), in which SR Ca channels function as a single uniform population of channels. They are not readily reconciled with the idea that SR Ca channels exist in two functionally distinct populations, voltage-gated and Ca-gated, and that only the Ca-gated channels are susceptible to Ca inactivation (Ríos, E., and G. Pizarro. 1988. *News in Physiological Sciences*. 3:223–227).

INTRODUCTION

In the normal activation of skeletal muscle, Ca ions are released from the sarcoplasmic reticulum (SR) into the myoplasmic solution where they can bind to the Ca-regulatory sites on troponin. In frog fibers, which were used for the experiments reported in this article, $\sim 300 \mu\text{M}$ Ca (referred to the myoplasmic solution) is released from the SR into the myoplasm after a single action potential (Baylor, Chandler, and Marshall, 1983; Baylor and Hollingworth, 1988; Pape, Jong, Chandler, and Baylor, 1993). This release is sufficient to complex most of the Ca-regulatory sites on troponin, as expected from the changes in intensity of the second actin layer line of the x-ray diffraction pattern (Kress, Huxley, Faruqi, and Hendrix, 1986). It is also sufficient to complex most of the Ca,Mg sites on parvalbumin that are free of divalent cations before stimulation (Gillis, Thomason, Lefevre, and Kretsinger, 1982; Baylor et al., 1983). As a result, most of the $300 \mu\text{M}$ total Ca that is released is rapidly complexed by troponin and parvalbumin.

A small fraction (<0.1) of the released Ca appears as the spatially averaged myoplasmic free [Ca] transient, $\Delta[\text{Ca}]$. In cut muscle fibers, the mean peak value of $\Delta[\text{Ca}]$ estimated with purpurate-3,3' diacetic acid (PDAA) is $\sim 20 \mu\text{M}$ with a sample standard deviation of $4 \mu\text{M}$ (Table II in Hirota, Chandler, Southwick, and Waggoner, 1989). In intact fibers, it is $\sim 10 \mu\text{M}$ with a sample standard deviation of $2 \mu\text{M}$ (Table II in Konishi and Baylor, 1991).

Because different fibers may have different amounts of Ca inside their SR, the question arises how are fibers able to release a relatively constant amount of Ca—approximately equal to the concentrations of Ca-regulatory sites on troponin and Ca,Mg sites on parvalbumin that are free of divalent cations before stimulation—and to have $\Delta[\text{Ca}]$ signals of approximately constant amplitude. One way to achieve such regulation is for the release process itself to sense the amplitude and duration of the increase in myoplasmic-free [Ca] and to inhibit additional release once the increase in [Ca] has been sufficient to insure that Ca has been bound to the readily available sites on troponin and parvalbumin (Baylor et al., 1983; Simon, Schneider, and Szúcs, 1985; Schneider and Simon, 1988; Simon, Klein, and Schneider, 1991). This inhibitory process will be called Ca inactivation of Ca release.

The experiments described in this article were undertaken to study this inactivation in cut muscle fibers that contain millimolar concentrations of EGTA (Pape, Jong, and Chandler, 1995) or fura-2 (Pape et al., 1993). Under these conditions, the amplitude of the spatially averaged $\Delta[\text{Ca}]$ signal is reduced and the increase in

myoplasmic free [Ca] during release is expected to be restricted to distances no greater than a few hundred nanometers of the SR release sites (Pape et al., 1995). In spite of these restrictions, Ca inactivation of Ca release appeared to be prominent in our experiments.

There are at least two advantages of the use of millimolar concentrations of a high affinity Ca buffer to study Ca inactivation of Ca release. Firstly, estimation of SR Ca release is direct: nearly all of the released Ca is captured by the buffer and its amount is determined from an associated optical change. In the experiments with EGTA, the change in pH that accompanies Ca complexation is monitored (Pape et al., 1995) whereas, in the fura-2 experiments, the change in Ca-free fura-2 concentration is monitored (Pape et al., 1993). Secondly, within a few milliseconds after cessation of a brief stimulation (e.g., that produced by an action potential or a 10–15-ms voltage-clamp pulse to -20 mV), $\Delta[\text{Ca}]$ decreases rapidly to a low value, barely above the prestimulus level, so that continued development of Ca inactivation of Ca release is minimized and the time course of recovery from inactivation can be measured unambiguously.

In most of our experiments, Ca inactivation of Ca release was produced by a first or conditioning stimulation and its effect was assessed by the change in Ca release elicited by a second stimulation. The inactivation had two main effects. The first is a reduction in the peak rate of SR Ca release (even after correction for the effects of Ca depletion), as first described by Simon et al. (1985) and Schneider and Simon (1988). The second effect, which is a new finding, is an alteration of the time course of release: its time to half peak is delayed and the initial rising phase is reduced. This reduction is sufficiently marked to indicate that most of the ability of the SR to release Ca, at least 0.9, is inactivated by a brief stimulation. Although we have no direct evidence that Ca causes these effects, such a causal action is certainly plausible because the reduction in the peak rate of release is similar to that attributed to Ca inactivation of Ca release in fibers with unmodified [Ca] transients (Simon et al., 1985; Schneider and Simon, 1988). Moreover, as shown in the Discussion, these effects on both the amplitude and time course of Ca release are expected from the model of Ca inactivation of Ca release proposed by Schneider and Simon (1988). For this reason, most of the effects of inactivation on Ca release described in this article will be interpreted as Ca inactivation of Ca release.

A preliminary report of some of these results was presented to the Biophysical Society (Jong, Pape, Baylor, and Chandler, 1994).

METHODS

The experiments were carried out at Yale University School of Medicine (New Haven, CT) on cut muscle fibers (Hille and Campbell, 1976) from cold-adapted *Rana temporaria*. The fibers were mounted in a double Vaseline-gap chamber (Kovács, Ríos, and Schneider, 1983; Irving, Maylie, Sizto, and Chandler, 1987), stretched to a sarcomere length of 3.4–4.2 μm , and studied at 14–15°C with the experimental methods used previously in this laboratory. The optical apparatus and method for the estimation of indicator-related absorbance signals are described in Irving et al. (1987) and Maylie, Irving, Sizto, and Chandler (1987). Methods for measurements with purple-3,3'-diacetic acid (PDAA) are described in Hirota et al. (1989). Methods with EGTA-phenol

red are described in the preceding article (Pape et al., 1995) and those with fura-2, in Pape et al. (1993). The electrical methods used for the measurement of intramembranous charge movement are described in Chandler and Hui (1990) and Hui and Chandler (1990, 1991). The holding potential was -90 mV.

The composition of the Ringer's solution that was used in the central pool in the action-potential experiments is the same as that given in Irving et al. (1987) and Pape et al. (1993). The compositions of the external solutions used in the central pool for the voltage-clamp experiments are given in Table I. The compositions of the internal solutions for both the action-potential and voltage-clamp experiments are given in Table II.

After a tetanus or voltage-clamp depolarization that depleted the SR of most of its readily releasable Ca, a 5-min period of recovery was usually used before the next stimulation. A recovery period of 3 min was usually used after a single action potential, two action potentials, or a pair of brief voltage-clamp depolarizations.

TABLE I
Composition of External Solutions in the Voltage-clamp Experiments

	TEA-gluconate	TEA-methane-sulfonate	TEA-MOPS	MgSO ₄	CaCl ₂
	<i>mM</i>				
TEA-gluconate	110	0	10	10	0
TEA-methanesulfonate	0	117	10	0	1.8

TEA and MOPS represent tetraethylammonium and 3-[*N*-Morpholino]propanesulfonic acid, respectively. Both solutions contained $1 \mu\text{M}$ tetrodotoxin and had a pH of 7.1. The TEA-gluconate solution is the same as that used in Pape et al. (1995). The TEA-methanesulfonate solution is the same as that used in Jong et al. (1993).

TABLE II
Composition of Internal Solutions

	X-glutamate	X ₂ -EGTA	Ca-EGTA	MgSO ₄	Y ₂ -ATP	X ₂ -CP	X ₃ -PEP	MOPS
	<i>mM</i>							
Action potential solutions								
(X = K; Y = Na):								
K-glutamate with 20 mM EGTA	45	18.24	1.76	6.8	5.5	20.0	5.0	5.0
K-glutamate	76	0.1	0	6.8	5.5	20.0	5.0	5.0
Voltage-clamp solutions								
(X = Y = Cs):								
Cs-glutamate with 20 mM EGTA	48	18.24	1.76	6.8	5.5	20.0	4.5	5.0
Cs-glutamate	76	0.1	0	6.8	5.5	20.0	4.5	5.0

EGTA, CP, and PEP represent ethyleneglycol-bis-(β -aminoethyl ether)-*N,N*-tetraacetic acid, creatine phosphate, and phospho(enol)pyruvate, respectively. The pH was adjusted to 7.0 by the addition of KOH to the action potential solutions or CsOH to the voltage clamp solutions. The calculated concentrations of free Mg and, in the solutions containing 20 mM EGTA, Ca were 1 mM and $0.036 \mu\text{M}$, respectively. The K- and Cs-glutamate solutions with 20 mM EGTA are the same as those used by Pape et al. (1995). The K- and Cs-glutamate solutions (with only 0.1 mM EGTA) are the same as those used by Pape et al. (1993) and Jong et al. (1993), respectively.

Statistical Tests of Significance

The difference between the mean values of two sets of results was assessed with Student's two-tailed *t* test and considered to be significant if $P < 0.05$.

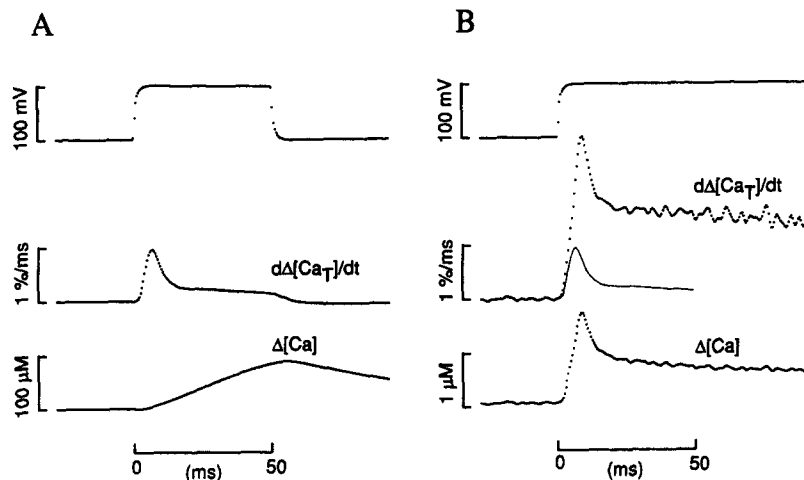


FIGURE 1. Ca signals during a voltage step to 10 mV for two conditions, for fibers equilibrated with 0.1 mM EGTA (*A*) and 20 mM EGTA (*B*). The traces in each panel show, from top to bottom, voltage, $d\Delta[\text{Ca}_T]/dt$, and $\Delta[\text{Ca}]$; the $d\Delta[\text{Ca}_T]/dt$ traces have been corrected for SR Ca depletion to give the fractional rates of release. (*A*) Average of four traces from the four fibers from *Rana temporaria* studied by Jong et al. (1993). The $\Delta[\text{Ca}]$ signal was measured with PDAA and the $d\Delta[\text{Ca}_T]/dt$ signal was calculated from it with model 1 in Table I of Pape et al. (1993). For the calculation, the myoplasmic concentration of Ca-regulatory sites on troponin was taken as 240 μM , the apparent dissociation constant as 2 μM , the forward rate constant as $0.575 \times 10^8 \text{ M}^{-1}\text{s}^{-1}$, and the backward rate constant as 115 s^{-1} ; the concentration of Ca,Mg sites on parvalbumin was taken as 1.5 mM, the dissociation constant for Ca as 4 nM (with the forward rate constant equal to $1.25 \times 10^8 \text{ M}^{-1}\text{s}^{-1}$ and the backward rate constant equal to 0.5 s^{-1}), and the dissociation constant for Mg as 91 μM (with the forward rate constant equal to $3.3 \times 10^4 \text{ M}^{-1}\text{s}^{-1}$ and the backward rate constant equal to 3.0 s^{-1}). To reduce noise in the $\Delta[\text{Ca}]$ and $d\Delta[\text{Ca}_T]/dt$ traces, the prestimulus baseline of the PDAA-related $\Delta\Delta(570)$ signal was set equal to its mean value. Interval of time between data points, 0.48 ms. The TEA-methanesulfonate solution was used in the central pool and the Cs-glutamate solution with PDAA was used in the end pools. (*B*) The $d\Delta[\text{Ca}_T]/dt$ and $\Delta[\text{Ca}]$ signals were estimated with EGTA-phenol red, as described in Pape et al. (1995). The $d\Delta[\text{Ca}_T]/dt$ signal during the period of depolarization in *A* is redrawn as a thin continuous curve in *B*. Fiber reference, 314921; time after saponin treatment of the end pool segments, 90 min; sarcomere spacing, 3.5 μm ; fiber diameter, 109 μm ; holding current, -39 nA; temperature, 14°C; concentration of phenol red at the optical site, 1.227 mM; estimated pH_R and free $[\text{Ca}]_R$, 6.855 and 0.061 μM , respectively; $[\text{Ca}_{\text{SR}}]_R$, 2,749 μM ; interval of time between data points, 0.48 ms. The TEA-methanesulfonate solution was used in the central pool and the Cs-glutamate solution with 20 mM EGTA plus 1.76 mM Ca and 0.63 mM phenol red was used in the end pools. The $\Delta[\text{Ca}]$ signals are displayed at different gains in *A* and *B*. In this and the following figures, 0 ms on the time axis corresponds to the start of the stimulus.

RESULTS

Ca inactivation of SR Ca Release During a Depolarization in Voltage-clamped Muscle Fibers Equilibrated with 0.1 mM EGTA

Fig. 1 A shows traces associated with a 50-ms depolarization from a holding potential of -90 mV to 10 mV. Each trace represents the average of four traces obtained from four different cut muscle fibers. The external solution contained TEA methanesulfonate and the internal solution contained Cs glutamate and a small concentration of EGTA, 0.1 mM, as is usually used in experiments on cut fibers. The top trace shows the voltage recorded in end pool 1. The bottom trace shows the free $[Ca]$ transient that was measured with PDAA, an indicator that is expected to provide a reliable estimate of both the time course and amplitude of the free $[Ca]$ transient (Hirota et al., 1989). Within a few milliseconds after depolarization, the $\Delta[Ca]$ signal began to increase. This increase continued until soon after repolarization to -90 mV when a maximal value of $88 \mu\text{M}$ was reached.

In the experiments reported in this article, $\Delta[Ca_T]$ is used to denote the amount of Ca released from the SR into the myoplasm, expressed in terms of myoplasmic concentration. In each of the four fibers used for Fig. 1 A, the time course of $\Delta[Ca_T]$ (not shown) was calculated from $\Delta[Ca]$ with the method described by Baylor et al. (1983). Briefly, numerical integration was used to give the time courses of $[Ca_{\text{Trop}}]$ (the myoplasmic concentration of Ca bound to the Ca-regulatory sites on troponin) and $[Ca_{\text{Parv}}]$ (the myoplasmic concentration of Ca bound to the Ca,Mg sites on parvalbumin). $\Delta[Ca_T]$ was then calculated from the equation $\Delta[Ca_T] = \Delta[Ca] + \Delta[Ca_{\text{PDAA}}] + \Delta[Ca_{\text{Trop}}] + \Delta[Ca_{\text{Parv}}]$, in which Δ denotes changes with respect to the resting levels; as discussed at the end of this section, the concentration of Ca that is removed by the SR Ca pump has not been included in the estimates of $\Delta[Ca_T]$. The parameters for the calculations of $\Delta[Ca_T]$, which were taken from model 1 in Table I in Pape et al. (1993), are given in the legend of Fig. 1.

The middle trace in Fig. 1 A shows the time course of $d\Delta[Ca_T]/dt$, averaged from the four fibers after correction for SR Ca depletion. For the correction procedure, each uncorrected value of $d\Delta[Ca_T]/dt$ was divided by the corresponding value of the readily releasable Ca inside the SR, $[Ca_{\text{SR}}]$ (expressed in terms of myoplasmic concentration), and multiplied by 100 to give units of percent/millisecond ($\%/ms$). The value of $[Ca_{\text{SR}}]$ was calculated from the equation $[Ca_{\text{SR}}] = [Ca_{\text{SR}}]_R - \Delta[Ca_T]$, in which the value of $[Ca_{\text{SR}}]_R$, the prestimulus value of $[Ca_{\text{SR}}]$, was taken from the first entry in column 7 of Table IIIA in Jong, Pape, Chandler, and Baylor (1993); its mean value is $4,938 \mu\text{M}$. If the SR Ca channels have a single conducting state with a Ca flux that is directly proportional to $[Ca_{\text{SR}}]$, the value of $d\Delta[Ca_T]/dt$ expressed in units of percent/millisecond should be directly proportional to the fraction of SR Ca channels that are open. Additional information about the depletion correction procedure, which was used for all of the $d\Delta[Ca_T]/dt$ signals that were recorded under voltage-clamp conditions in this article, is given in Jong et al. (1993) and in the text discussion of Fig. 13 in Pape et al. (1995).

The $d\Delta[Ca_T]/dt$ signal in Fig. 1 A increased rapidly after depolarization and, at 6.6 ms, reached a peak value of $0.96 \%/ms$. At the time of the peak, the value of $\Delta[Ca]$ was $4.4 \mu\text{M}$. During the next 10 ms, as $\Delta[Ca]$ continued to increase, the

$d\Delta[\text{Ca}_T]/dt$ signal decreased rapidly to a quasi-steady level of 0.23 %/ms, determined in the interval 20–30 ms after depolarization. The time constant of the final half of the decrease was 3.2 ms. This rapid decrease in the rate of SR Ca release is presumed to be due to Ca inactivation of Ca release (Baylor et al., 1983; Simon et al., 1985; Schneider and Simon, 1988; Simon et al., 1991).

The values of the parameters given in the preceding paragraph were obtained from the signals in Fig. 1 A, which were averaged from four fibers from *Rana temporaria*. Mean values and SEM's from the four individual fibers are 0.998 %/ms (SEM, 0.208 %/ms) for the peak rate of release, 0.227 %/ms (SEM, 0.039 %/ms) for the quasi-steady rate of release, and 2.66 ms (SEM, 0.43 ms) for the time constant.

The ratio of the quasi-steady to peak value of $d\Delta[\text{Ca}_T]/dt$ provides some, although probably not direct, information about the fraction of SR Ca channels that were not inactivated during the depolarization. The mean value was 0.232 (SEM, 0.016) in the four fibers from *Rana temporaria* that were used for Fig. 1 A. In three other fibers, from *Rana pipiens*, it was 0.181 (SEM, 0.010) (Table III in Jong et al., 1993).

In Fig. 1 A, the use of $d\Delta[\text{Ca}_T]/dt$ to estimate the rate of SR Ca release should be considered to be only approximate for two reasons. Firstly, the reliability of the calculation depends on the reliability of the values of the concentrations of troponin and parvalbumin and of their association and dissociation rate constants with Ca and, in the case of parvalbumin, Mg. Because the values of these parameters (given in the legend of Fig. 1) were determined from biochemical and morphological measurements, as described in Baylor et al. (1983), it is necessary to assume that the same values apply inside a muscle fiber. Since it has not been possible to verify this assumption experimentally, its use introduces an uncertainty into the estimation of $d\Delta[\text{Ca}_T]/dt$. A definite advantage of the EGTA-phenol red method, which is used in the rest of this article, is that the measurement of $d\Delta[\text{Ca}_T]/dt$ is direct so that this uncertainty is avoided.

Secondly, the calculation of $d\Delta[\text{Ca}_T]/dt$ does not take into account the amount of Ca that is removed from the myoplasm by the SR Ca pump, both by binding and by translocation. Our method to estimate these amounts was described previously (Pape, Konishi, Hollingworth, and Baylor, 1990; Jong et al., 1993) and is based on the 11-step reaction cycle for the pump proposed by Fernandez-Belda, Kurzmack and Inesi (1984). Calculations with this method show that, in Fig. 1 A, the peak and quasi-steady rates of SR Ca release should be 1.09 and 0.36 %/ms, respectively, rather than 0.96 and 0.23 %/ms based on $d\Delta[\text{Ca}_T]/dt$ alone. Another advantage of the EGTA-phenol red method for the measurement of SR Ca release is that changes in free [Ca] are small so the rate of binding and translocation of Ca by the SR Ca pump is expected to be small and negligible compared with $d\Delta[\text{Ca}_T]/dt$.

Ca Inactivation of SR Ca Release during a Depolarization in Voltage-clamped Muscle Fibers Equilibrated with 20 mM EGTA

The traces in Fig. 1 B are analogous to those in Fig. 1 A except that the fiber had been equilibrated for 1.5 h with an end-pool solution that contained 20 mM EGTA with 1.76 mM Ca and 0.63 mM phenol red. The computational procedure de-

scribed in the preceding article (Pape et al., 1995) was used to estimate $\Delta[\text{Ca}]$ from the phenol red signal. As in Fig. 1 A and throughout this article, the $\Delta[\text{Ca}]$ signal represents the spatially averaged change in myoplasmic free $[\text{Ca}]$. In the presence of a large concentration of EGTA, however, the increase in $[\text{Ca}]$ during release is expected to be restricted to distances within a few hundred nanometers of the SR Ca release sites (Pape et al., 1995).

In Fig. 1 B, the composition of the external solution and the amplitude of the depolarization, 10 mV, were the same as those used in the experiments in Fig. 1 A. For the first 4–5 ms after the depolarization, the time course of the $d\Delta[\text{Ca}_T]/dt$ signal in Fig. 1 B is similar to but slightly above that in Fig. 1 A, which is indicated by a continuous curve (drawn only during the period of depolarization). Thereafter, the signals diverge markedly as $d\Delta[\text{Ca}_T]/dt$ in Fig. 1 B continued to increase and to eventually reach a peak value that was slightly more than three times that in Fig. 1 A. This comparison suggests that, at the time of the peak value of $d\Delta[\text{Ca}_T]/dt$ in Fig. 1 A, the activation of the SR Ca channels had not reached a steady level and Ca inactivation of Ca release was developing rapidly. As a result, fewer than half the SR Ca channels were actually open at the time of the peak rate of release in Fig. 1 A.

After the $d\Delta[\text{Ca}_T]/dt$ signal in Fig. 1 B reached a peak value of 3.01 %/ms, it decreased to a quasi-steady level of 1.62 %/ms (determined 20–44 ms after depolarization) with a final time constant of 3.73 ms. In another fiber studied under similar conditions (fiber 316921), the peak value was 1.71 %/ms, the quasi-steady value was 1.12 %/ms, and the final time constant was 6.12 ms. Thus, on average, the peak value of $d\Delta[\text{Ca}_T]/dt$ with 20 mM EGTA was 2.36 %/ms (SEM, 0.65 %/ms), the quasi-steady value was 1.37 %/ms (SEM, 0.25 %/ms), and the final time constant was 4.93 ms (SEM, 1.20 ms). For comparison, the corresponding mean values from the four fibers with 0.1 mM EGTA that were used in Fig. 1 A were 0.998%/ms, 0.227%/ms, and 2.66 ms (given above). The peak of the $\Delta[\text{Ca}]$ signal in the experiment in Fig. 1 B and in the other experiment with 20 mM EGTA was reduced by two orders of magnitude compared with that in Fig. 1 A (note different gains).

These results are consistent with the idea that EGTA reduced myoplasmic free $[\text{Ca}]$ and that this, in turn, reduced Ca inactivation of Ca release. Nevertheless, Ca inactivation of Ca release appears to have developed in the presence of millimolar concentrations of EGTA, as evidenced by the rapid decline of the $d\Delta[\text{Ca}_T]/dt$ signal in Fig. 1 B from the peak to the quasi-steady level, a decline that is qualitatively similar to that observed in Fig. 1 A. Since the onset of inactivation also appears to have developed rapidly in Fig. 1 B, it seems unlikely that all of the SR Ca release channels were open at the peak of the $d\Delta[\text{Ca}_T]/dt$ signal.

In the experiment in Fig. 1 B, the quasi-steady value of $d\Delta[\text{Ca}_T]/dt$ divided by the peak value was 0.537. In another similar experiment with EGTA (fiber 316921), a value of 0.657 was obtained. The mean of these values, 0.597 (SEM, 0.060), is significantly different from those obtained from fibers from *Rana temporaria* and *Rana pipiens* equilibrated with only 0.1 mM EGTA, 0.232 and 0.181, respectively (given above).

Our results obtained from fibers with unmodified $[\text{Ca}]$ transients (Fig. 1 A and related experiments) can be compared with the results obtained by Schneider and Simon (1988) under similar conditions. Our mean values of the quasi-steady to

peak ratio of $d\Delta[\text{Ca}_T]/dt$, 0.23 from *Rana temporaria* and 0.18 from *Rana pipiens*, are similar to their range of values, 0.2–0.3 from *Rana pipiens*. On the other hand, our mean values of the final time constant, 2.66 ms (SEM, 0.09 ms) from *Rana temporaria* and 1.58 ms (SEM, 0.08 ms) from *Rana pipiens*, are very much smaller than their mean value from *Rana pipiens*, 32.3 ms (SEM, 1.9 ms).

We do not have a satisfactory explanation for such a marked difference in the values of the final time constant. Some of the differences in the two sets of experiments are: (a) the method used to estimate SR Ca release, (b) the temperature (Schneider and Simon [1988] worked at 6–10°C whereas we used 14°C), and (c) the range of voltages (Schneider and Simon [1988] used depolarizations to –41 to –20 mV whereas we used 10 mV). It seems unlikely that the range of voltages can account for the difference, however, because the time constant appears to be independent of membrane potential between –41 and 0 mV (Melzer, Ríos, and Schneider, 1984; Schneider and Simon, 1988).

The general conclusion from experiments such as those used for Fig. 1 is that equilibration of a fiber with 20 mM EGTA and 1.76 mM Ca reduces the amount of Ca inactivation of Ca release that develops during a step depolarization (as evidenced by increases in both the peak and quasi-steady values of $d\Delta[\text{Ca}_T]/dt$). 20 mM EGTA, however, does not completely eliminate Ca inactivation of Ca release (as evidenced by a quasi-steady to peak ratio of $d\Delta[\text{Ca}_T]/dt$ that is less than unity). Other experiments also suggest that the amount of Ca inactivation of Ca release that remains after equilibration with 20 mM EGTA is little affected by whether the external solution contains 1.8 mM Ca or 10 mM Mg: for example, the $d\Delta[\text{Ca}_T]/dt$ signal in Fig. 1 *B* is very similar to that in Fig. 13 of Pape et al. (1995).

Ca Inactivation of Ca Release Studied with Action-potential Stimulation

It was also of interest to characterize the amount of Ca inactivation of Ca release that is produced by an action potential in fibers equilibrated with 20 mM EGTA. As shown in the following section, the time course of recovery from this inactivation can be used to estimate the amount of inactivation that develops during an action potential and is present immediately afterward.

Schneider and Simon (1988) were the first investigators to study the time course of recovery of Ca inactivation of Ca release. They used voltage-clamp stimulation of cut fibers that were equilibrated with an internal solution that contained only a small concentration of EGTA, 0.1 mM. SR Ca release was measured during two depolarizing pulses, a prepulse and a test pulse. Inactivation was elicited by the prepulse and the time course of its recovery was estimated with test pulses applied after different periods of repolarization.

Schneider and Simon (1988) found that, after repolarization, recovery began only after free [Ca] had decayed to near its prestimulus level. After a sufficiently long period of repolarization, the peak rate of SR Ca release recovered to a new constant level that was smaller than that obtained without a prepulse, a finding attributed to SR Ca depletion (Schneider, Simon, and Szűcs, 1987). The time constant of recovery to the new level was, on average, 90 ms at 6–10°C. Schneider and Simon (1988) regarded this value as an upper limit of the time constant of recovery

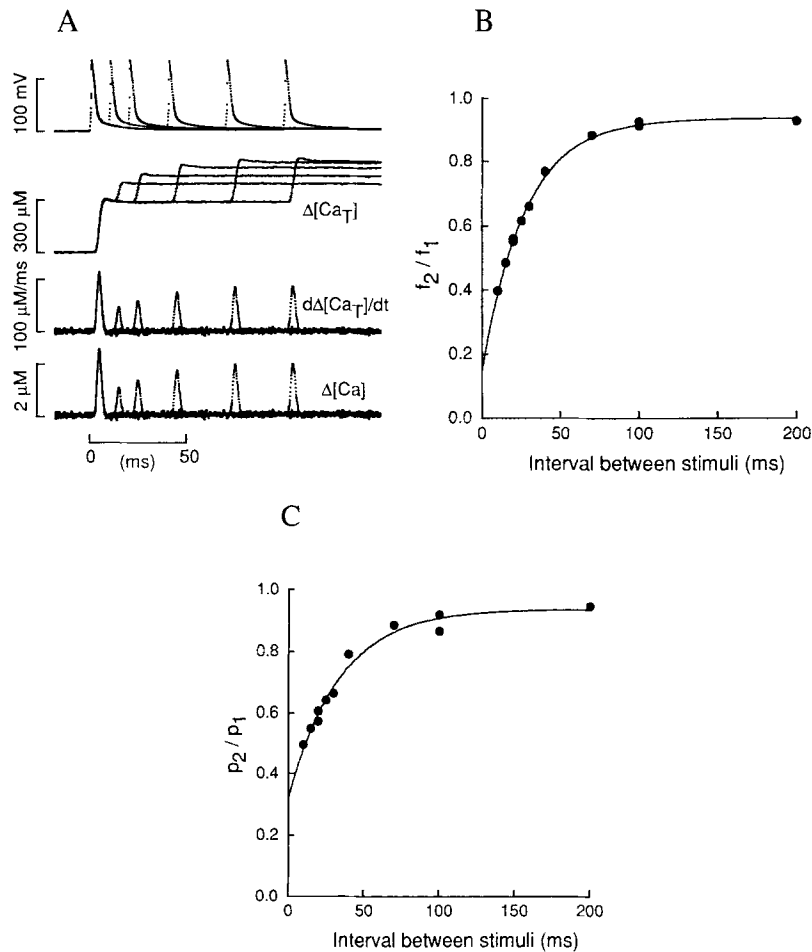


FIGURE 2. SR Ca release elicited by two action potentials separated by interstimulus intervals of varying duration. (A) The top set of superimposed traces shows five pairs of action potentials in which the second action potential was stimulated 10–100 ms after the first. The first action potentials of each pair essentially coincide. The next sets of superimposed traces show, in order, the corresponding $\Delta[\text{Ca}_T]$, $d\Delta[\text{Ca}_T]/dt$, and $\Delta[\text{Ca}]$ signals. (B) The filled circles show the values of f_2/f_1 plotted as a function of the interval between the initiation of the two stimuli. For each value of f_2 and f_1 , $\Delta[\text{Ca}_T]$ was averaged during the interval 10–13 ms after the stimulus; this interval was chosen so that the final part of the signal after the first action potential could be resolved when the interval between stimuli was as short as 10 ms, the shortest interval used. The continuous curve shows the exponential function plus a constant that was least-squares fitted to the experimental points. It is equal to 0.151 at 0 ms and 0.281 at 5 ms and approaches a final value of 0.939; the time constant is 27.5 ms. (C) Similar to B except that the filled circles show the values of p_2/p_1 . The fitted exponential curve is equal to 0.322 at 0 ms and 0.408 at 5 ms and approaches a final value of 0.935; the time constant is 33.1 ms. Fiber reference, O10911; time after saponin treatment, 77–110 min; sarcomere spacing, 3.4 μm ; fiber diameter, 130 μm ; holding current, -46 to -47 nA; amplitude of first action potential, 132 mV; temperature, 15°C; concentration of phenol red at the optical site, 1.098–1.468 mM; esti-

at resting free [Ca], however, because the value of free [Ca] was elevated during the first part of the recovery period.

Schneider and Simon (1988) also found that, if the prepulse produced only partial inactivation, inactivation continued to develop during the period of repolarization for as long as the value of free [Ca] remained elevated. As these authors pointed out, this observation provides good evidence that the inactivation is Ca dependent. Unfortunately, it is not easy to obtain similar evidence in our experiments because the Ca buffering action of EGTA or fura-2 rapidly reduced the value of free [Ca] during the recovery period to just above the prestimulus level. On the other hand, this reduction in free [Ca] allows a straightforward estimate of the rate constant for recovery from Ca inactivation of Ca release.

Fig. 2 shows the results of an experiment in which recovery was studied with two action potentials. The external solution was Ringers and the internal solution was the K-glutamate solution with 20 mM EGTA plus 1.76 mM Ca and phenol red (Table II). The top superimposed traces in Fig. 2 A show five pairs of action potentials recorded with different intervals between the two stimuli. The second set of traces shows $\Delta[\text{Ca}_T]$. The responses associated with all of the first action potentials coincide, indicating that the condition of the fiber was stable throughout the experiment. The first responses rapidly increased to an early peak and then decreased slightly to a nearly constant steady level until the second period of release began. This steplike waveform is consistent with the idea that the duration of SR Ca release after an action potential is brief and that the rate with which Ca dissociates from CaEGTA and is returned to the SR is very slow (Pape et al., 1995). The third set of traces in Fig. 2 A shows $d\Delta[\text{Ca}_T]/dt$.

In Fig. 2 A, the amplitudes of the $\Delta[\text{Ca}_T]$ and $d\Delta[\text{Ca}_T]/dt$ signals associated with the second action potential were smaller than those associated with the first action potential. With the smallest interstimulus interval used, 10 ms, the second $\Delta[\text{Ca}_T]$ and $d\Delta[\text{Ca}_T]/dt$ signals were, respectively, only ~ 0.34 and 0.43 times the corresponding first signals. As the interval was increased, the amplitudes of both second signals increased, consistent with recovery from inactivation. The amplitudes after the longest recovery period, 100 ms, were smaller than those of the first signal, presumably because of SR Ca depletion (Schneider et al., 1987).

The changes in the amplitude of $\Delta[\text{Ca}_T]$ and $d\Delta[\text{Ca}_T]/dt$ after the second action potential in Fig. 2 A were accompanied by little if any change in the action potential waveform; the difference between the amplitudes of the first and second action potentials was 2.9 mV for an interstimulus interval of 10 ms and between 1.6 and -1.5 mV for intervals ≥ 15 ms.

mated pH_R and free $[\text{Ca}]_R$, 6.960–6.929 and 0.044–0.050 μM , respectively; interval of time between data points, 0.12 ms. The value of $[\text{Ca}_{SR}]_R$ was 1,781 μM 5 min before the first run of the series and 1,844 μM 10 min after the last run; the mean of these two values, 1,813 μM , was used for correcting the values of $\Delta[\text{Ca}_T]$ and $d\Delta[\text{Ca}_T]/dt$ for SR Ca content. The mean values of f_1 and p_1 were 0.164 and 6.12 %/ms, respectively. Ringer's solution was used in the central pool and the K-glutamate solution with 20 mM EGTA plus 1.76 mM Ca and 0.63 mM phenol red was used in the end pools.

The bottom trace in Fig. 2 A shows the $\Delta[\text{Ca}]$ signal. During each interstimulus interval, from the end of the first period of SR Ca release until the beginning of the second period, EGTA was able to buffer myoplasmic free $[\text{Ca}]$ to a small value that was only slightly above the resting level. During this period, any Ca that was bound to a putative inactivation receptor would have had a chance to dissociate and be bound by EGTA, thus removing its inactivating effect.

Pape et al. (1995) used f_n to represent the fractional amount of Ca released from the SR by the n^{th} action potential; its value is equal to the increase in total Ca concentration in the myoplasmic solution produced by the n^{th} action potential divided by the value of $[\text{Ca}_{\text{SR}}]$ just before the n^{th} action potential. Fig. 2 B shows the values

TABLE III
Recovery of SR Ca Release after an Action Potential in Fibers Equilibrated with 20 mM EGTA

(1)	(2)–(5)				(6)–(9)			
	f_2/f_1				p_2/p_1			
Fiber reference	Y(0)	Y(5)	Y(∞)	τ	Y(0)	Y(5)	Y(∞)	τ
	<i>ms</i>				<i>ms</i>			
425911	0.213	0.339	0.935	26.1	0.268	0.379	0.926	27.0
923911	0.148	0.279	0.997	29.8	0.234	0.349	0.900	26.4
925911	0.029	0.196	0.959	25.3	-0.012	0.175	0.951	23.1
O10911	0.151	0.281	0.939	27.5	0.322	0.408	0.935	33.1
Mean	0.135	0.274	0.958	27.2	0.203	0.328	0.928	27.4
SEM	0.038	0.029	0.014	1.0	0.074	0.052	0.011	2.1

Column 1 gives the fiber reference. A decreasing exponential function plus a constant was fitted to recovery data such as those illustrated in Fig. 2 B (for f_2/f_1) and Fig. 2 C (for p_2/p_1). Columns 2–4 give the values of the function fitted to f_2/f_1 at 0, 5, and ∞ ms, respectively; column 5 gives the values of the time constant of the exponential function. Columns 6–9 are analogous to columns 2–5 except that the values were obtained from the functions fitted to p_2/p_1 . Time after saponin treatment, 77–158 min; sarcomere spacing, 3.4–3.6 μm ; fiber diameter, 86–137 μm ; holding current, -33 to -77 nA; amplitude of the first action potential, 118–134 mV; temperature, 14–15°C; concentration of phenol red at the optical site, 0.903–1.804 mM; estimated pH_R and $[\text{Ca}]_R$, 6.844–6.960 and 0.044–0.074 μM ; SR Ca content, 1,813–2,562 μM . Ringer's solution was used in the central pool and the K-glutamate solution with 20 mM EGTA plus 1.76 mM Ca and 0.63 mM phenol red was used in the end pools.

of f_2/f_1 plotted as a function of the interval between stimuli. The curve represents a least-squares fit of a decreasing exponential function plus a constant. The curve has an initial value of 0.151 and approaches a steady state value of 0.939 with a time constant of 27.5 ms.

Fig. 2 C shows the values of p_2/p_1 plotted as a function of the interval between stimuli; p_n represents the peak value of $d\Delta[\text{Ca}_T]/dt$ elicited by the n^{th} action potential, divided by the value of $[\text{Ca}_{\text{SR}}]$ just before the n^{th} action potential and then multiplied by 100 to give units of percent/millisecond. The fitted exponential curve has an initial value of 0.322, a final value of 0.935, and a time constant of 33.1 ms.

Results similar to those in Fig. 2 were obtained in three other experiments in which recovery was measured after an action potential. Table III gives information about the exponential fits of the time courses of the recovery of f_2/f_1 and p_2/p_1 . Column 1 gives the fiber reference. Columns 2 and 4 give, respectively, the initial and final values of the exponential curves fitted to f_2/f_1 and column 5 gives the values of the time constant of the exponential function. Columns 6, 8, and 9 give similar information about the exponential fits to p_2/p_1 .

The mean values of the time constant for the recovery of f_2/f_1 and p_2/p_1 are 27.2 (column 5 in Table III) and 27.4 ms (column 9), respectively. These values are not significantly different from each other but are significantly smaller than the values of the recovery time constant obtained in voltage-clamp experiments, as discussed below in connection with Table IV.

The mean steady state values of the fitted recovery curves are 0.958 for f_2/f_1 (column 4 in Table III) and 0.928 for p_2/p_1 (column 8). Both values are close to unity, indicating that recovery was nearly complete. The second value, 0.928, is significantly smaller than unity, however, consistent with the idea that some of the inactivating effects of an action potential remain after a period of repolarization as long as 0.2 s. Similar long lasting effects were also observed after brief voltage-clamp pulses (Figs. 5, 6, and 8 and Table IV).

The Values of f_2/f_1 and p_2/p_1 without Recovery between the First and Second Action Potential Are Estimated to Be ~ 0.3

If the exponential curves in Fig. 2, *B* and *C*, are reliable monitors of the time course of recovery from inactivation, their initial values might be taken as estimates of the values of f_2/f_1 and p_2/p_1 that would have been obtained if there had been no recovery after the first action potential. It seems likely, however, that recovery occurred only during the period when the value of free [Ca] was small and near its prestimulus level, i.e., from the time when free [Ca] had returned to near the baseline level after the first action potential until the time when it started to increase after the second action potential (bottom trace in Fig. 2 *A*). This interval of time is shorter than the interstimulus interval by ~ 5 ms. Thus, more realistic estimates of the values of f_2/f_1 (Fig. 2 *B*) and p_2/p_1 (Fig. 2 *C*) without recovery are expected to be given by the values of the fitted curves at 5 ms. These are given in columns 3 and 7, respectively, in Table III. The mean values, 0.274 for f_2/f_1 and 0.328 for p_2/p_1 , are not significantly different from each other.

The main conclusion of this and the preceding section is that, immediately after an action potential in a fiber equilibrated with 20 mM EGTA and 1.76 mM Ca, a large fraction of the ability of the SR to release Ca appears to be inactivated, roughly 0.7 (one minus the values in columns 3 and 7 in Table III), and that, after free [Ca] is reduced to near its prestimulus level, this inactivation recovers with a time constant of ~ 25 ms (columns 5 and 9 in Table III). Another method for the estimation of the amount of inactivation produced by an action potential, described below, gives a value of at least 0.9.

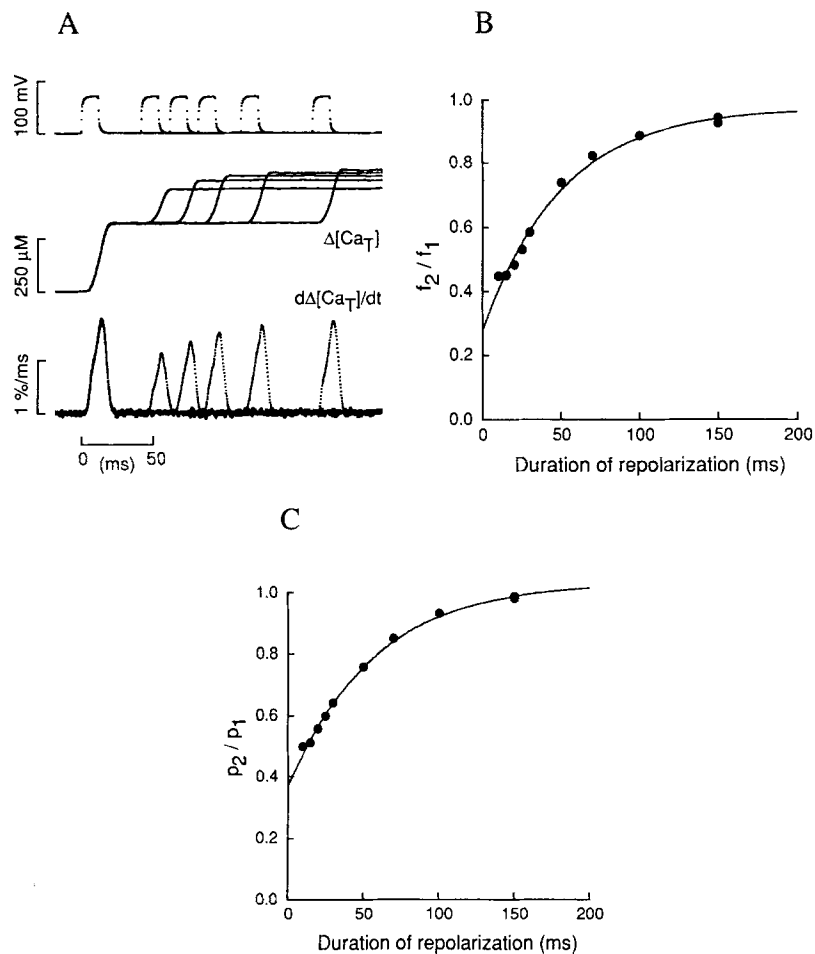


FIGURE 3. Voltage-clamp simulation of the two action-potential experiment in Fig. 2. SR Ca release was elicited by two 12-ms voltage pulses to -20 mV separated by a repolarization interval to -90 mV of varying duration. (A) The top set of traces shows five superimposed records of voltage. The middle and bottom sets of traces show, respectively, the corresponding $\Delta[Ca_T]$ and $d\Delta[Ca_T]/dt$ signals. (B) The filled circles show the values of f_2/f_1 plotted as a function of the duration of repolarization. The continuous curve shows the exponential function plus a constant that was least-squares fitted to the experimental points. Its initial and final values are 0.280 and 0.976, respectively, and its time constant is 50.5 ms. (C) Similar to B except that the filled circles show the values of p_2/p_1 . The fitted exponential curve has initial and final values of 0.370 and 1.036 and a time constant of 57.2 ms. Fiber reference, N26911; time after saponin treatment, 163–190 min; sarcomere spacing, 3.4 μm ; fiber diameter, 129–130 μm ; holding current, -44 nA; temperature, $14^\circ C$; concentration of phenol red at the optical site, 1.846–1.925 mM; estimated pH_R and free $[Ca]_R$, 6.822–6.803 and 0.082–0.090 μM , respectively; interval of time between data points, 0.24 ms. The value of $[Ca_{SR}]_R$ was 1,986 μM 5 min before the first run of the series and 2,171 μM 3 min after the last run; linear interpolation was used to estimate values during the series. The mean values of f_1 and p_1 were 0.157 and 1.78 %/ms, respectively. The TEA-gluconate solution was used in the central pool and the Cs-glutamate solution with 20 mM EGTA plus 1.76 mM Ca and 0.63 mM phenol red was used in the end pools. In this and subsequent figures, the $d\Delta[Ca_T]/dt$ signals have been corrected for SR Ca depletion.

Two Brief Voltage Pulses Can Be Used to Study the Recovery of Ca Inactivation of Ca Release

The next experiments were carried out to find out whether the marked degree of inactivation produced by an action potential in fibers equilibrated with 20 mM EGTA could also be observed with brief depolarizations in a voltage-clamp experiment.

Fig. 3 shows the results of an experiment carried out on a fiber equilibrated with the Cs-glutamate internal solution with 20 mM EGTA plus 1.76 mM Ca and phenol red; the external solution was TEA-gluconate (with 10 mM Mg and nominally 0 mM Ca). The top superimposed traces show five voltage records, each taken with two 12-ms pulses to -20 mV that were separated by periods of repolarization that varied from 30 to 150 ms. The duration of the depolarization was selected so that the mean value of f_1 (0.157 in Fig. 3) would be similar to that in the action-potential experiments (0.164 in Fig. 2). (f_1 , f_2 , p_1 , and p_2 have meanings that are similar to those used in the action-potential experiments.) The pulse duration was too brief, however, for $d\Delta[\text{Ca}_T]/dt$ to reach a peak value during either the first or second pulse.

The middle and bottom sets of traces in Fig. 3 A show $\Delta[\text{Ca}_T]$ and $d\Delta[\text{Ca}_T]/dt$, respectively. The $d\Delta[\text{Ca}_T]/dt$ traces have been corrected for SR Ca depletion, as was routinely done in experiments on voltage-clamped fibers. The $\Delta[\text{Ca}]$ traces (not shown) have the same waveform as the $d\Delta[\text{Ca}_T]/dt$ traces, similar to the situation in Fig. 2 A. In this experiment, as in the one in Fig. 2 A, all of the $\Delta[\text{Ca}_T]$ and $d\Delta[\text{Ca}_T]/dt$ signals associated with the first pulse, or prepulse, were similar. The signals elicited by the second pulse, or test pulse, however, were small when the duration of repolarization was brief, and their amplitudes progressively increased as the duration was increased.

Fig. 3, B and C, shows the values of f_2/f_1 (B) and p_2/p_1 (C) plotted as a function of the duration of repolarization. The curve in each panel shows a least-squares fit of a decreasing exponential function plus a constant to the data. In B, the initial and final values of the curve are 0.280 and 0.976, respectively, and the time constant of the exponential function is 50.5 ms. In C, the initial and final values are 0.370 and 1.036 and the time constant is 57.2 ms. These results are generally similar to those obtained with action-potential stimulation, as illustrated in Fig. 2, except that the value of the time constant of recovery is about twice as large.

Voltage-clamp results, similar to those in Fig. 3, were obtained in a total of five experiments in which SR Ca release was monitored with two brief (10–15 ms) pulses to -20 mV separated by a variable period of repolarization. The first five rows in Table IV give the parameters associated with the fitted exponential curves from these experiments. Column 1 gives the fiber reference. Columns 2 and 3 give, respectively, the initial and final values of each curve fitted to f_2/f_1 and column 4 gives the values of the time constant of the exponential function. Columns 5–7 give similar information for the curves fitted to p_2/p_1 . All of the values of the mean and SEM at the bottom of the table were calculated from the data in these first five rows. The data in the last two rows of the table were not used for the means because they give values of parameters obtained with a brief prepulse and a long lasting test pulse, as described in the next section.

In these experiments, the rate of Ca release increased after depolarization with a delay that was approximately equal to the time required for release to turn off after repolarization. Consequently, the duration of repolarization was approximately equal to the period of time during which SR Ca release, and consequently the value of myoplasmic free [Ca], was small and close to the prestimulus level. For this reason, the initial values of the exponential curves fitted to f_2/f_1 and p_2/p_1 in Table IV are expected to represent the values that would have been obtained if no recovery

TABLE IV
Recovery of SR Ca Release after a Brief Depolarization in Fibers Equilibrated with 20 mM EGTA

(1)	Ratio of rising phases											
	f_2/f_1			p_2/p_1			Prepulse			Test (150 ms)		
	Y(0)	Y(∞)	τ	Y(0)	Y(∞)	τ	Y(0)	Y(∞)	τ	Y(0)	Y(∞)	τ
			<i>ms</i>			<i>ms</i>			<i>ms</i>			<i>ms</i>
N14911	0.183	0.985	38.9	0.267	0.979	37.2	0.013	0.810	46.2	-0.028	1.041	38.5
N15911	0.201	0.986	44.7	0.275	1.036	49.1	0.067	0.825	50.6	0.052	1.050	47.0
N19911	0.445	0.994	49.6	0.524	0.974	62.4	0.248	0.773	38.6	0.337	1.024	37.1
N25911	0.368	0.970	31.5	0.507	0.964	37.1	0.046	0.799	60.3	0.100	1.256	98.1
N26911	0.280	0.976	50.5	0.370	1.036	57.2	0.093	0.796	42.7	0.169	1.050	50.6
N25911				0.586	1.002	56.4	-0.082	0.726	40.7	-0.198	1.015	35.4
N26911				1.030	1.403	73.2	0.117	0.796	43.7	0.127	1.037	39.5
Mean	0.295	0.982	43.0	0.389	0.998	48.6	0.093	0.801	47.6	0.126	1.084	54.3
SEM	0.050	0.004	3.5	0.055	0.016	5.1	0.041	0.009	3.7	0.062	0.043	11.2

Column 1 gives the fiber reference. A decreasing exponential function plus a constant was fitted to recovery data such as those illustrated in Fig. 3 B for f_2/f_1 , Figs. 3 C and 6 A for p_2/p_1 , Fig. 6 C for the ratio of the initial rising phases of the test and prepulse $d\Delta[Ca_T]/dt$ signals, and Fig. 6 D for the ratio of the initial rising phases of the test and 150 ms recovery test $d\Delta[Ca_T]/dt$ signals. Columns 2 and 3 give the values of the function fitted to f_2/f_1 at 0 and ∞ ms, respectively; column 4 gives the values of the time constant of the exponential function. Columns 5-7, 8-10, and 11-13 are analogous to 2-4 except that the functions were fitted to p_2/p_1 , the ratio of the initial rising phases of the test and prepulse signals, and the ratio of the initial rising phases of the test and 150-ms recovery test signals, respectively. The values in the first five rows were obtained with 10-15 ms test pulses that had the same duration as the prepulses; only these values were used for the determination of the Mean and SEM. The values in rows 6 and 7 were obtained with 250-ms test pulses. All prepulses and test pulses were to -20 mV. Time after saponin treatment 68-207 min; sarcomere spacing, 3.4 μ m; fiber diameter, 84-149 μ m; holding current, -24 to -73 nA; temperature, 14°C; concentration of phenol red at the optical site, 0.969-1.950 mM; estimated pH_R and $[Ca]_R$, 6.797-6.888 and 0.060-0.092 μ M; SR Ca content, 1,996-2,759 μ M. The TEA-gluconate solution was used in the central pool and the Cs-glutamate solution with 20 mM EGTA plus 1.76 mM Ca and 0.63 mM phenol red was used in the end pools.

from inactivation had occurred after the prepulse. These values should be compared with the corresponding 5-ms values of the curves that were fitted in the action-potential experiments, columns 3 and 7 in Table III. For f_2/f_1 , these values were 0.295 (SEM, 0.050) in the voltage-clamp experiments (column 2 in Table IV) and 0.274 (SEM, 0.029) in the action-potential experiments (column 3 in Table III); the difference is not significant. For p_2/p_1 , these values were 0.389 (SEM,

0.055) in the voltage-clamp experiments (column 5 in Table IV) and 0.328 (SEM, 0.052) in the action-potential experiments (column 7 in Table III); this difference is also not significant.

In the voltage-clamp experiments, the mean value of the time constant for the recovery of f_2/f_1 , 43.0 ms (SEM, 3.5 ms; column 4 in Table IV), is not significantly different from that for p_2/p_1 , 48.6 ms (SEM, 5.1 ms; column 7 in Table IV). Both values are significantly larger than the corresponding values in the action-potential experiments, 27.2 ms (SEM, 1.0 ms) for f_2/f_1 (column 5 in Table III) and 27.4 ms (SEM, 2.1 ms) for p_2/p_1 (column 9 in Table III). The reason for this difference is not known but may be related to the presence of different univalent cations in the internal solutions in the action-potential (K^+) and voltage-clamp (Cs^+) experiments (Table II).

The mean value of the time constant associated with p_2/p_1 in our voltage-clamp experiments, 48.6 ms, is smaller than the mean value obtained by Schneider and Simon (1988) in voltage-clamp experiments on cut fibers equilibrated with a Cs-glutamate solution that contained only 0.1 mM EGTA, 90 ms (SEM, 10 ms). These authors, however, considered 90 ms to represent an upper limit of the actual value of the time constant for Ca dissociation from its putative receptor, because free [Ca] was elevated during the early part of the recovery period in their experiments. In addition, their time constants would be expected to be somewhat larger than ours because their experiments were carried out at 6–10°C whereas the experiments in Table IV were carried out at 14°C.

The main conclusion from these experiments is that, in a fiber equilibrated with 20 mM EGTA and 1.76 mM Ca, a substantial amount of Ca inactivation of Ca release appears to develop after a brief voltage-clamp pulse to -20 mV (Fig. 3 and Table IV, columns 1–7), similar to the inactivation that develops after an action potential (Fig. 2 and Table III).

Both the Amplitude and Time Course of SR Ca Release Are Affected by Ca Inactivation of Ca Release

Additional information about recovery from Ca inactivation of Ca release can be obtained by increasing the duration of the test pulse so that the entire time course of $d\Delta[Ca_T]/dt$ can be resolved, as was done by Schneider and Simon (1988). Fig. 4 A shows traces from an experiment in which a 12-ms prepulse to -20 mV was followed by a 20 ms repolarization to -90 mV and then a 250-ms test pulse to -20 mV; the solutions are the same as those used in the experiments in Fig. 3 and Table IV. The top trace shows voltage and the next three traces show, in order, $\Delta[Ca_T]$, $d\Delta[Ca_T]/dt$, and $\Delta[Ca]$. The $\Delta[Ca_T]$ trace shows that the prepulse released $450 \mu M$ Ca from the SR into the myoplasm. During the period of repolarization, after SR Ca release had stopped, the $\Delta[Ca_T]$ signal was constant. This constancy is similar to that observed after the first stimulations in Figs. 2 A and 3 A and is attributed to the slow rate with which Ca dissociates from CaEGTA and returns to the SR. During the test pulse, $\Delta[Ca_T]$ increased to a final level of $2,299 \mu M$. This value is taken to be equal to $[Ca_{SR}]_R$.

In this experiment, the duration of the prepulse was sufficiently long for the $d\Delta[Ca_T]/dt$ signal to reach a peak value, $2.89 \%/ms$, during the pulse and to show

a partial decline before repolarization. The signal had a smaller peak during the test pulse, 2.08 %/ms, consistent with the development of Ca inactivation of Ca release during the prepulse and incomplete recovery during the period of repolarization. The quasi-steady value of the test pulse signal, after the peak, was 1.46 %/ms. The final portion of the signal has not been plotted because of the noise introduced by the correction for SR Ca depletion.

The quasi-steady to peak ratio of $d\Delta[\text{Ca}_T]/dt$ in Fig. 4 *A* can be estimated from the quasi-steady level during the test pulse and the peak value during the prepulse,

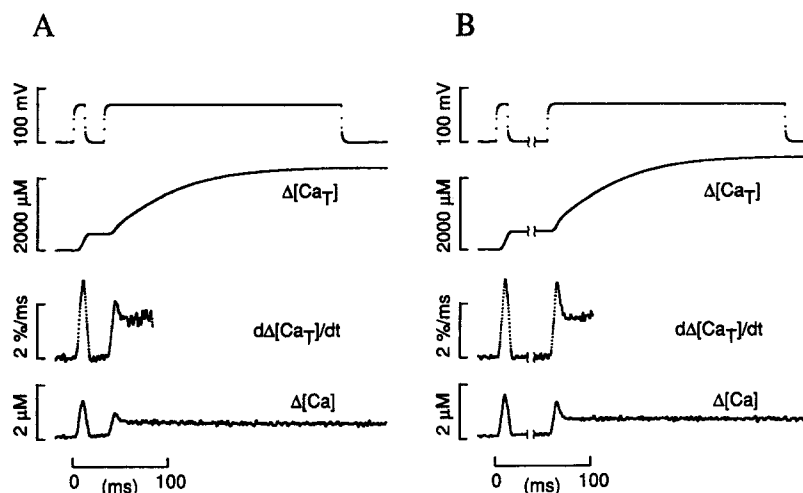


FIGURE 4. Ca signals recorded during a two pulse voltage-clamp experiment, with a long test pulse. The pulse protocol was a 12-ms prepulse to -20 mV, a 20 (*A*) or 150 (*B*) ms repolarization to -90 mV, and a 250-ms test pulse to -20 mV. The traces in each panel show, from top to bottom, voltage, $\Delta[\text{Ca}_T]$, $d\Delta[\text{Ca}_T]/dt$, and $\Delta[\text{Ca}]$. In *B*, a section of each trace has been deleted between the two vertical wavy lines. Fiber reference, N25911; sarcomere spacing, $3.4 \mu\text{m}$; temperature, 14°C ; interval of time between data points, 0.24 ms. The two illustrated trials were taken from an experiment with the following range of values: time after saponin treatment of the end pool segments, 122–172 minutes; fiber diameter, 86–88 μm ; holding current, -26 nA; concentration of phenol red at the optical site, 1.315–1.546 mM; estimated pH_R and free $[\text{Ca}]_R$, 6.820–6.823 and $0.082 \mu\text{M}$, respectively; $[\text{Ca}_{\text{SR}}]_R$, 2,566–2,129 μM . The TEA-gluconate solution was used in the central pool and the Cs-glutamate solution with 20 mM EGTA plus 1.76 mM Ca and 0.63 mM phenol red was used in the end pools.

$1.463/2.888 = 0.507$. This ratio was determined in 10 other runs in this fiber. The mean value from all 11 runs was 0.518 (SEM, 0.003). This value is somewhat smaller than, but not significantly different from, the mean values obtained with single depolarizations in other fibers that had also been equilibrated with 20 mM EGTA: 0.60 (SEM, 0.04; two fibers) for a step depolarization to 60 mV with the TEA-gluconate external solution (Pape et al., 1995) and 0.60 (SEM, 0.06; two fibers) for a step depolarization to 10 mV with the TEA-methanesulfonate external solution (Fig. 1 *B* and another fiber).

Fig. 4 *B* shows a similar set of traces obtained with a 150 ms period of repolarization. Pairs of wavy vertical lines indicate where a section of each trace has been deleted during the recovery period. The main difference between the $d\Delta[\text{Ca}_T]/dt$ signals in Fig. 4, *A* and *B*, is that the amplitude of the test signal in Fig. 4 *B* had recovered to near its prepulse value.

In Fig. 4 *B*, the time constant of the final decay of the test $d\Delta[\text{Ca}_T]/dt$ signal from its peak to quasi-steady value was 2.02 ms. The mean value of the time constant from four such determinations on this fiber was 2.41 ms (SEM, 0.27 ms). Similar traces were analyzed in four other fibers. The mean value of the time constant from all five fibers was 1.87 ms (SEM, 0.60 ms). This value, obtained at -20 mV, is not significantly different from that obtained with single depolarizations to 60 mV with the same external solution, 3.33 ms (SEM, 0.23 ms; two fibers) (Pape et al., 1995),

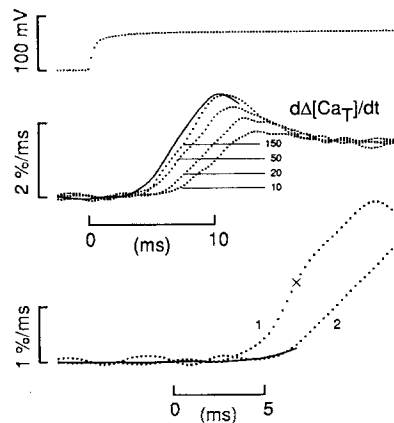


FIGURE 5. Effect of the duration of repolarization on the $d\Delta[\text{Ca}_T]/dt$ signal during a test pulse, from the experiment in Fig. 4. The top trace shows a single test voltage. The middle continuous curve shows $d\Delta[\text{Ca}_T]/dt$ averaged during four 12-ms prepulses; the trace has been translated so that the beginning of the prepulse coincides with the beginning of the test pulse. The superimposed dotted traces show $d\Delta[\text{Ca}_T]/dt$ during the test pulses, with repolarization times indicated (in milliseconds). The two dotted traces at the bottom show $d\Delta[\text{Ca}_T]/dt$ signals during the prepulse (labeled 1) and test pulse (2) from the trial with a 20-ms repolarization time, plotted with

an expanded gain and time base. Trace 1 was least-squares fitted to trace 2 from the beginning of the trace to the time to half peak, indicated by an x . The continuous curve shows the fit, given by scaling trace 1 by the factor 0.171. Additional information is given in the legend of Fig. 4.

or from that obtained with single depolarizations to 10 mV when the external solution was TEA-methanesulfonate, 4.93 ms (SEM, 1.20 ms; Fig. 1 *B* and another fiber).

The top trace in Fig. 5 shows the voltage during the first part of the test pulse plotted on an expanded time scale, from the experiment illustrated in Fig. 4. The middle set of traces shows superimposed $d\Delta[\text{Ca}_T]/dt$ signals. The continuous trace shows the average of four signals during the prepulse, shifted in time so that the initiation of the prepulse coincides with that of the test pulse. The dotted traces show four individual test signals that were preceded by different periods of repolarization, as indicated (in milliseconds). When the period of repolarization was short, the peak amplitude of the test $d\Delta[\text{Ca}_T]/dt$ signal was smaller than that of the prepulse. As the period of repolarization was increased, the amplitude progressively increased. These observations about the recovery of the amplitude of

$d\Delta[\text{Ca}_T]/dt$ are similar to those made by Schneider and Simon (1988) in cut fibers in which the myoplasmic free $[\text{Ca}]$ transient had not been attenuated by EGTA.

The dotted middle traces in Fig. 5 also show a result that is not apparent in the records of Schneider and Simon (1988) and Simon et al. (1991): the reduction in

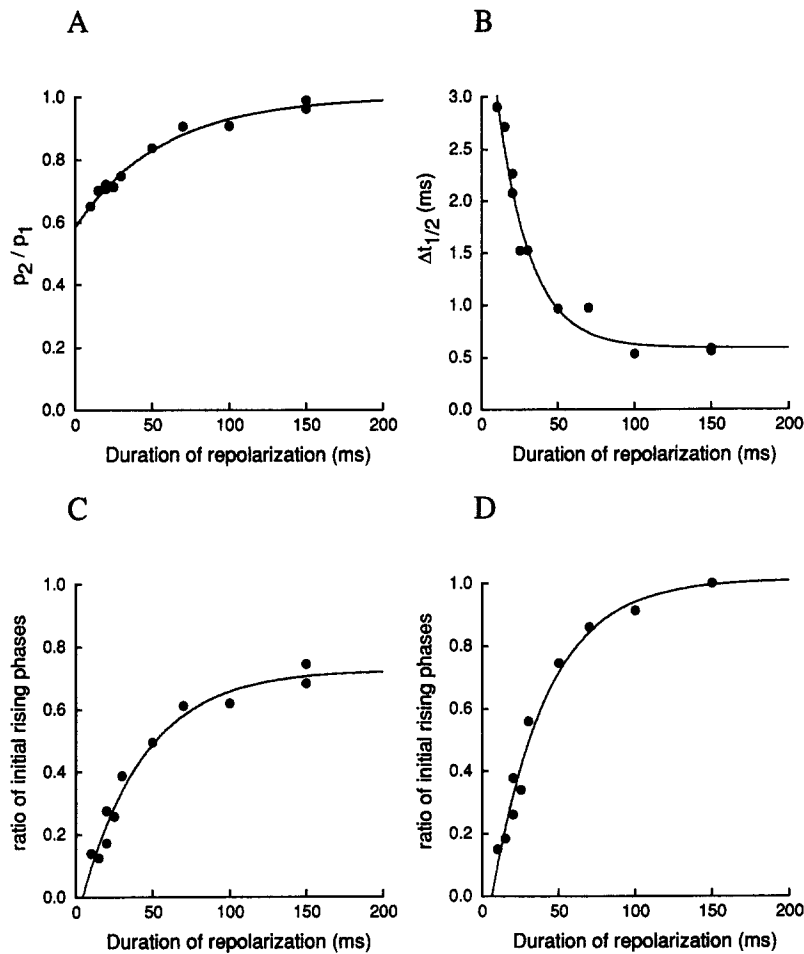


FIGURE 6. Effect of the duration of repolarization on some of the parameters associated with the $d\Delta[\text{Ca}_T]/dt$ signal, from the experiment in Figs. 4–5. Each continuous curve represents a least-squares fit of a decreasing exponential function plus a constant to the data. (A) p_2/p_1 : the curve has initial and final values of 0.586 and 1.002, respectively; the time constant of the exponential function is 56.4 ms. (B) $\Delta t_{1/2}$: the curve has initial and final values of 4.43 and 0.59 ms, respectively; the time constant of the exponential function is 21.5 ms. (C) the ratio of the initial rising phases of the test and prepulse $d\Delta[\text{Ca}_T]/dt$ signals: the curve has initial and final values of -0.082 and 0.726 , respectively; the time constant of the exponential function is 40.7 ms. (D) the ratio of the initial rising phases of the test and 150-ms recovery test $d\Delta[\text{Ca}_T]/dt$ signals: the curve has initial and final values of -0.198 and 1.015 , respectively; the time constant of the exponential function is 35.4 ms. Additional information is given in the legend of Fig. 4.

peak amplitude of $d\Delta[\text{Ca}_T]/dt$ was associated with a delay in the time to half peak of the signal and a corresponding increase in the time to peak. A small delay appeared to remain in the $d\Delta[\text{Ca}_T]/dt$ signal even after a 150-ms repolarization, although the peak amplitude of the signal had recovered almost completely. This long lasting delay was a consistent finding in all of our experiments.

The filled circles in Fig. 6 A show the values of p_2/p_1 from the experiment in Fig. 5, plotted as a function of the duration of repolarization; p_1 and p_2 represent the peak values of $d\Delta[\text{Ca}_T]/dt$, in units of percent/millisecond, elicited by the first and second voltage pulses, respectively. For brief periods of repolarization, the values of p_2/p_1 in Fig. 6 A are larger than those in Fig. 3 C. This difference probably arises because the long test pulse used in the experiment in Fig. 6 A allowed $d\Delta[\text{Ca}_T]/dt$ to reach its peak value, even after brief periods of repolarization when the time to peak was delayed. The continuous curve in Fig. 6 A shows a decreasing exponential function plus a constant that was least-squared fitted to the data. The initial and final values of the curve are 0.586 and 1.002, respectively, and the time constant of the exponential function is 56.4 ms; these values are given in columns 5–7 of Table IV in the sixth row (labeled N25911). The initial value, 0.586, is slightly larger than the mean value of the ratio of quasi-steady to peak $d\Delta[\text{Ca}_T]/dt$ that was estimated in the same experiment, 0.518 (given above, in the discussion of Fig. 4).

Another parameter that was used to assess the recovery of the $d\Delta[\text{Ca}_T]/dt$ signal in Fig. 5 is $\Delta t_{1/2}$, the difference in the times to half-peak of the test pulse and prepulse $d\Delta[\text{Ca}_T]/dt$ signals, each determined with respect to the initiation of the depolarization. Fig. 6 B shows $\Delta t_{1/2}$ plotted as a function of the duration of repolarization. The initial and final values of the fitted exponential curve are 4.43 and 0.59 ms, respectively. The time constant of the exponential function is 21.5 ms, which is only ~ 0.4 times that in Fig. 6 A. It is difficult to interpret this difference, however, because of nonlinearities that probably exist between the value of $\Delta t_{1/2}$ and the extent of Ca inactivation (see below). At 100 and 150 ms, both the data and the curve have values of 0.5–0.6 ms, suggesting that recovery has a slow as well as a rapid phase and that complete recovery requires a period of repolarization that is longer than 0.2 s.

This was the only experiment in which both the prepulse and test pulse were sufficiently long for the peak value of $d\Delta[\text{Ca}_T]/dt$ to be determined during both pulses. Consequently, this was the only experiment in which the time to half peak of the signal could be determined during both pulses so that a value of $\Delta t_{1/2}$ could be obtained. Similar test-pulse delays were consistently observed in our other experiments, however, although reliable estimates of $\Delta t_{1/2}$ could not be made.

A Brief Prepulse Inactivates Almost All of the Ability of the SR to Release Ca

The $d\Delta[\text{Ca}_T]/dt$ traces in Fig. 5 were also analyzed in terms of their initial rising phases. Let r denote the fraction of the SR Ca release mechanism that is in the non-inactivated state just before a prepulse. $(1 - r)$, then, is the fraction that is in the inactivated state. Let $\gamma_R(t)$ and $\gamma_I(t)$ represent the time courses of the rate of SR Ca release that would be observed during depolarization with the initial condition $r = 1$ and 0, respectively. An example of $\gamma_R(t)$ and $\gamma_I(t)$, based on the model of Ca inactivation of Ca release proposed by Schneider and Simon (1988), is shown in Fig. 12,

in which $y_R(t)$ and $y_I(t)$ are represented by the $f(t)$ traces labeled 1 and 0, respectively.

To a first approximation, for any value of r between 0 and 1, the time course of $d\Delta[Ca_T]/dt$ after a depolarization is expected to be given by

$$d\Delta[Ca_T]/dt = (ry)_R(t) + (1-r)y_I(t). \quad (1)$$

This equation relies on the assumption that $y_R(t)$ and $y_I(t)$ are uniquely determined waveforms that are independent of r . It seems likely that this assumption might hold during the first few milliseconds of a depolarization, when SR Ca release is just beginning. At later times, however, the assumption may fail because the time course of SR Ca release and, thus, its effect on Ca inactivation of release may vary according to the value of r .

Traces 1 and 2 at the bottom of Fig. 5 show $d\Delta[Ca_T]/dt$ signals that were obtained, respectively, during a prepulse and during a test pulse after a 20-ms period of repolarization; trace 1 has been shifted in time so that the initiation of the prepulse coincides with that of the test pulse. The amplitude and time scale are different from those used for the middle traces. Trace 1 was scaled to give a least-squares fit to trace 2 during the interval from the beginning of the trace to its half peak, marked by an x . The continuous curve shows the fit, determined by a scaling factor of 0.171.

Let r_p and r_T denote the values of r just before the prepulse and test pulse, respectively. If $y_I(t) \cong 0$ during the period used for the fit, it follows from Eq. 1 that r_T/r_p is equal to the scaling factor 0.171. If the assumption that $y_I(t) \cong 0$ does not hold, and $y_I(t) > 0$ during part of this period, the value of r_T/r_p would be expected to be < 0.171 . Effects of the inequality $y_I(t) > 0$ can be seen in the model calculations in Fig. 12, in which the initial part of the $f(t)$ trace labeled 0 (which corresponds to the $y_I(t)$ trace) is fitted by 0.103 times the $f(t)$ trace labeled 1 (which corresponds to the $y_R(t)$ trace). Thus, in general, the scaling factor 0.171 implies that, at the beginning of pulse 2, at most, 0.171 of the SR Ca release mechanism was in the same state that it was in at the beginning of pulse 1. Consequently, at least 0.829 of the release mechanism that was in the resting state before the prepulse had been altered, presumably inactivated, by the prepulse and had failed to recover during the 20-ms period of repolarization that separated the prepulse and test pulse.

One advantage of the use of scaling factors to describe the effect of a prepulse on the time course of $d\Delta[Ca_T]/dt$ is that the values of the scaling factor and of r_T/r_p are expected to be related in an approximately linear manner. Consequently, during recovery, if the value of r_T increases along an exponential time course, the scaling factor is expected to increase according to the same exponential function. This is not the case when the effect of a prepulse is analyzed in terms of $\Delta t_{1/2}$, as was done in Fig. 6 B, or in terms of some other temporal parameter such as the latency of $d\Delta[Ca_T]/dt$ (not shown). The reason is that the value of such a temporal parameter is not related in a linear way to r_T .

Fig. 6 C shows the scaling factors that were obtained with the fitting procedure illustrated at the bottom of Fig. 5, plotted as a function of the duration of repolarization. The initial and final values of the fitted exponential curve are -0.082 and

0.726, respectively, and the time constant of the exponential function is 40.7 ms; these values are given in columns 8–10 of Table IV in the sixth row (labeled N25911).

The results in Fig. 6 C and Table IV show three features of interest. Firstly, although the curve in Fig. 6 C may not be very accurate because of noise in the data, the initial value -0.082 suggests that most of the ability of the SR to release Ca had been inactivated by the brief depolarizing prepulse. The mean initial value from five experiments is 0.093 (column 8 in Table IV). If the extrapolation of the exponential recovery curve to zero time is valid, this value indicates that, on average, at least $0.907 (= 1 - 0.093)$ of the ability of the SR to release Ca had been inactivated by the prepulse.

Secondly, the time constants of the recovery of p_2/p_1 and of the the ratio of the rising phases are similar. In Fig. 6 A, the time constant of the exponential function is 56.4 ms whereas, in Fig. 6 C, it is 40.7 ms. Although these values are somewhat different from each other, the mean values from the five fibers in Table IV are not significantly different: the time constants of the recovery of p_2/p_1 and of the the ratio of the rising phases are 48.6 ms (SEM, 5.1 ms; column 7) and 47.6 ms (SEM, 3.7 ms; column 10), respectively. This similarity is consistent with the idea that the same inactivation mechanism is responsible for both the reduction in amplitude of the $d\Delta[\text{Ca}_T]/dt$ signal and the delay in its time to half-peak. By analogy with the results of Schneider and Simon (1988), this mechanism is expected to be Ca inactivation of Ca release.

Thirdly, the final level of the curve in Fig. 6 C, 0.726, and the mean final level in column 9 of Table IV, 0.801, are less than unity, suggesting again that recovery from the effects of a brief prepulse has both a rapid and a slow phase and that complete recovery requires a repolarization longer than 0.2 s. It seems likely that the underlying mechanism is the same as that of the long lasting increase in $\Delta t_{1/2}$ that was observed in Fig. 6 B. It is not known whether the slowly recovering component of inactivation is due to Ca inactivation of Ca release or to some other process (see Discussion).

To assess the effect of the rapidly recovering component of Ca inactivation of Ca release on the $d\Delta[\text{Ca}_T]/dt$ signal, the scaling procedure illustrated at the bottom of Fig. 5 was repeated with the 150-ms test $d\Delta[\text{Ca}_T]/dt$ signal instead of the prepulse $d\Delta[\text{Ca}_T]/dt$ signal (not shown). Fig. 6 D shows the scaling factors, plotted and fitted in a manner similar to that shown in Fig. 6 C. The initial and final values of the curve are -0.198 and 1.015 , respectively, and the value of the time constant of the exponential function is 35.4 ms. These values are given in columns 11–13 of Table IV in the sixth row (labeled N25911). The results in Fig. 6 D and columns 11–13 of Table IV are similar to those in Fig. 6 C and columns 8–10 of Table IV except that the steady state values are near unity. The mean initial value of 0.126, given in column 11 in Table IV, indicates that, on average, at least $0.874 (= 1 - 0.126)$ of the ability of the SR to release Ca had been affected by the rapidly recovering component of Ca inactivation of Ca release immediately after the prepulse.

Another fiber (N26911) was also studied with the combination of a short prepulse and long test pulse separated by a variable period of repolarization. Exponential time courses were fitted to recovery data such as those shown in Fig. 6, A, C, and

D; the values of the fitted parameters are given in the seventh row of columns 5–13 of Table IV. In this experiment, the duration of the prepulse was too short for the $d\Delta[\text{Ca}_T]/dt$ signal to reach a peak. Consequently, the values of $\Delta t_{1/2}$ could not be determined and both the initial and final values of the fitted curve through the p_2/p_1 data (columns 5 and 6 in Table IV) were unusually large.

The main conclusion of this section is that a 10–15-ms prepulse to -20 mV appears to inactivate most of the ability of the SR to release Ca. If the extrapolation of the exponential recovery curve to zero time is valid (Fig. 6, *C* and *D*), the fractional inactivation is at least 0.9. It will be shown in the Discussion that such a large fractional inactivation is consistent with the large relative difference between the time constants associated with the decay of the $d\Delta[\text{Ca}_T]/dt$ signal to its quasi-steady level, ~ 2 – 4 ms, and with the recovery from inactivation, ~ 50 ms in the voltage-clamp experiments reported in this article.

An Action Potential Also Appears to Inactivate Almost All of the Ability of the SR to Release Ca

The $d\Delta[\text{Ca}_T]/dt$ signals in the action-potential experiments in Table III were also examined for any decreases in the initial rising phase elicited by the second action potential. The plots of scaling factor against interval between stimuli (not shown) were noisy but consistently showed changes that were qualitatively similar to those illustrated in Fig. 6 *C*. The mean value of the fitted exponential curves at 5 ms, 0.086 (SEM, 0.081), is similar to, and not significantly different from, the comparable mean value in column 8 in Table IV, 0.093 (SEM, 0.041). The mean final value of the fitted curves, 0.744 (SEM, 0.068), is also similar to, and not significantly different from, the mean final value in column 9 in Table IV, 0.801 (SEM, 0.009). The mean time constant of the exponential functions in the fit was 29.3 ms (SEM, 4.4 ms); this value is not significantly different from those in columns 5 and 9 of Table III, 27.2 and 27.4 ms, respectively, but is significantly smaller than the analogous time constant observed in the voltage-clamp experiments, 47.6 ms (column 10 of Table IV). Thus, within the resolution of the data, the decrease in the initial rising phase of the $d\Delta[\text{Ca}_T]/dt$ signal in the action-potential experiments was as marked as that in the voltage-clamp experiments.

Intramembranous Charge Movement Is Little Affected by Ca Inactivation of Ca Release

Simon et al. (1991) found that Ca inactivation of Ca release, produced by a prepulse, was not associated with a reduction in the amount of intramembranous charge that moved during a test pulse. Because our results show that a prepulse is also able to delay the time to half peak of SR Ca release, it seemed important to find out whether the time to half peak of intramembranous charge movement is delayed.

Fig. 7 shows traces from the same fiber used for the experiment in Fig. 4. In this run, however, the prepulse and test pulse had not only the same amplitude, -20 mV, but also the same duration, 12 ms; the repolarization interval was 20 ms. The

top trace shows the voltage. The next two traces show the current from intramembranous charge movement, I_{cm} , and its running integral, Q_{cm} , which represents the cumulative amount of charge that had moved. The bottom trace shows $d\Delta[Ca_T]/dt$.

Fig. 8 A shows the same traces as Fig. 7 except that the prepulse responses (labeled 1) have been shifted 32 ms along the time axis so that they can be compared directly with the test pulse responses (labeled 2). The two voltage traces are essentially identical, as expected. The two traces of I_{cm} , second row, are similar except (a) just before the test pulse, trace 2 was below trace 1 (because trace 2 was still returning to baseline) and (b) 2–7 ms after the depolarization (i.e., the interval during the pulse just below the numeral 1), trace 1 was slightly above trace 2. Such differences are less marked in the traces of Q_{cm} (third row), which nearly coincide both during and after the pulses.

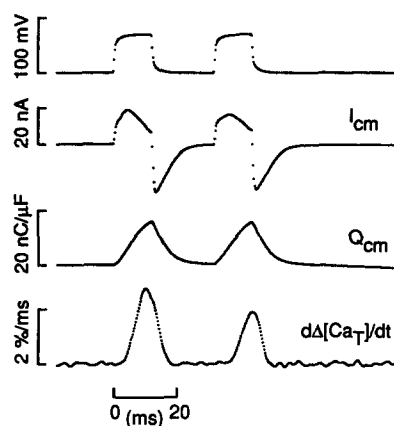


FIGURE 7. Intramembranous charge movement (I_{cm}) and $d\Delta[Ca_T]/dt$ during a brief prepulse and test pulse. The prepulse and test pulse were 12 ms depolarizations to -20 mV, separated by a 20-ms repolarization to -90 mV. The traces, from top to bottom, show voltage, I_{cm} , Q_{cm} , and $d\Delta[Ca_T]/dt$. Same fiber as used for Figs. 4–6. Time after saponin treatment of the end pool segments, 110 min; fiber diameter, 85 μ m; holding current, -25 nA; concentration of phenol red at the optical site, 1.242 mM; estimated pH_R and free $[Ca]_R$, 6.836 and 0.077 μ M, respectively; $[Ca_{SR}]_R$, 2,647 μ M; interval of time between data points, 0.24 ms. Additional information is given in the legend of Fig. 4.

The bottom traces in Fig. 8 A show $d\Delta[Ca_T]/dt$. Trace 2 is clearly different from trace 1: its time to half peak is delayed and its amplitude is reduced. Because these differences are much more marked than the relatively small differences in I_{cm} or Q_{cm} , it seems unlikely that the changes in the $d\Delta[Ca_T]/dt$ signal are due to changes in activation mediated by intramembranous charge movement. This conclusion also applies to Q_{cm} raised to the fourth power (not shown), which may be related to $d\Delta[Ca_T]/dt$ more directly than Q_{cm} raised to the first power (Simon and Hill, 1992).

Fig. 8 B shows a similar set of traces with a 150-ms repolarization interval. In this case, the I_{cm} and Q_{cm} traces were essentially identical whereas the test $d\Delta[Ca_T]/dt$ trace (labeled 2) was delayed ~ 0.5 ms with respect to the prepulse trace (labeled 1), similar to the delay between the prepulse trace and the trace labeled 150 in Fig. 5.

Two main conclusions follow from the experiment in Figs. 7 and 8 and other similar experiments. The first is that the delay in the time to half peak of $d\Delta[Ca_T]/dt$

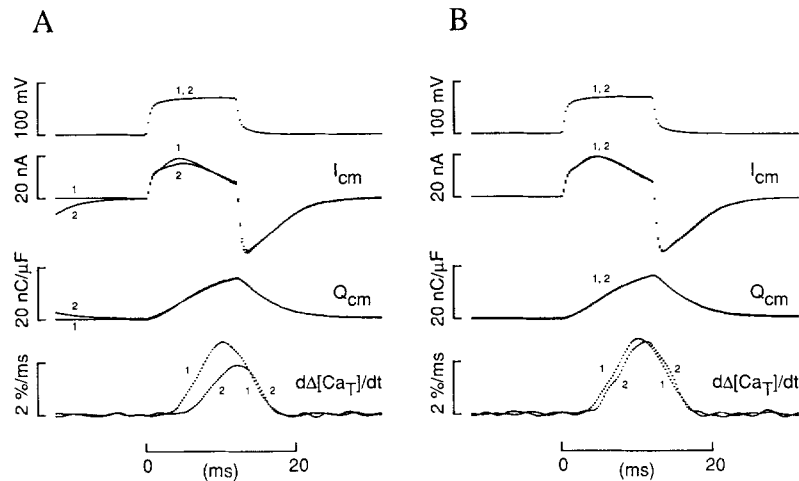


FIGURE 8. Comparison of the time course of intramembranous charge movement and $d\Delta[Ca_T]/dt$ during a brief prepulse (labeled 1) and test pulse (2) separated by a period of repolarization of 20 ms (A) and 150 ms (B). (A) The four pairs of traces are taken from Fig. 7 and are plotted on an expanded time scale in the same order from top to bottom. Each pair shows the signal during the prepulse superimposed with that during the test pulse; the prepulse signal has been translated along the time axis by an amount equal to the combined duration of the prepulse and repolarization interval. Additional information is given in the legends to Fig. 4 and 7. (B) Similar to A except that the traces were taken 9 min later with a repolarization interval of 150 ms. Time after saponin treatment of the end pool segments, 119 min; fiber diameter, 86 μ m; holding current, -26 nA; concentration of phenol red at the optical site, 1.301 mM; estimated pH_R and free $[Ca]_R$, 6.836 and 0.077 μ M, respectively; $[Ca_{SR}]_R$, 2,599 μ M. The other information is the same as that for Fig. 7.

produced by prepulse inactivation is not accompanied by any substantial change in charge movement; consequently, it seems likely that the delay is due to changes in the regulation of SR Ca release that occur after intramembranous charge movement. Secondly, if the activation of SR Ca release is to be explained quantitatively in terms of intramembranous charge movement, as has been attempted in several studies (Rakowski, Best, and James-Kracke, 1985; Melzer, Schneider, Simon and Szűcs, 1986; Simon and Schneider, 1988; Simon and Hill, 1992), it is important to allow for the effects exerted by Ca inactivation of Ca release on both the amplitude and the time course of the rate of release.

Ca Inactivation of Ca Release Is Not Prevented by Large Concentrations (6–8 mM) of Fura-2

Because fura-2 is able to bind Ca much more rapidly than EGTA, it would be expected to be more effective in reducing free $[Ca]$ during release and, consequently, more effective in reducing the development of Ca inactivation. According to Eq. A10 in Pape et al. (1995), spatially averaged $\Delta[Ca]$ in the EGTA experiments is approximately equal to $(k_1[EGTA]_R)^{-1}$ times the rate of SR Ca release; k_1 repre-

sents the association rate constant for Ca and EGTA. Appendices B and D in Pape et al. (1995) show that the same factor, $(k_1[\text{EGTA}]_R)^{-1}$, determines the ability of EGTA to reduce local increases in free $[\text{Ca}]$ near SR release sites. Because a similar factor, $(k_2[\text{fura-2}]_R)^{-1}$, is expected to apply to experiments in which an excess concentration of fura-2 is used, spatially averaged $\Delta[\text{Ca}]$ and local $\Delta[\text{Ca}]$ should be reduced to the same extent by EGTA and fura-2 if $k_1[\text{EGTA}]_R = k_2[\text{fura-2}]_R$; k_2 represents the association rate constant for Ca and fura-2. With $k_1 = 2.5 \times 10^6 \text{ M}^{-1}\text{s}^{-1}$, $[\text{EGTA}]_R = 18.24 \text{ mM}$ (Pape et al., 1995), and $k_2 = 0.7 \times 10^8 \text{ M}^{-1}\text{s}^{-1}$ (the value measured with 2 mM fura-2, Pape et al., 1993), it follows that 0.65 mM fura-2 is expected to reduce $\Delta[\text{Ca}]$ (both the spatially averaged $\Delta[\text{Ca}]$ signal and local $\Delta[\text{Ca}]$) to the same extent as 18.24 mM EGTA (20 mM total EGTA with 1.76 mM Ca), at least if only small amounts of Ca are released from the SR. Since concentrations of fura-2 as large as 8 mM were used in some of our previous experiments (Pape et al., 1993; Jong et al., 1993), it was of interest to find out whether such large concentrations of fura-2 could prevent some of the effects attributed to Ca inactivation of Ca release that are observed with 20 mM EGTA. In the interpretation of the results presented in this section, it is important to bear in mind that fura-2, at large con-

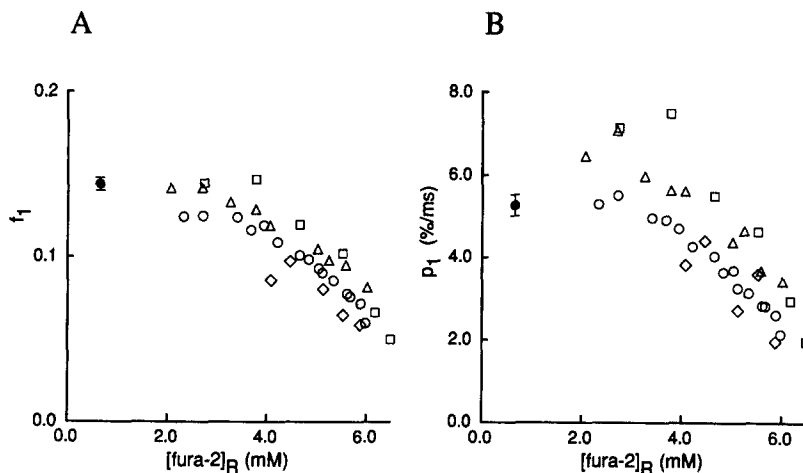


FIGURE 9. Effect of $[\text{fura-2}]_R$ on f_i (A) and p_1 (B) in action-potential stimulated fibers. The open symbols show values obtained from four fibers exposed to the K-glutamate solution with 8 mM fura-2 plus 0–2 mM Ca. The filled symbols show the mean values (with \pm SEM bars) from 12 fibers equilibrated with K-glutamate with 20 mM EGTA plus 1.76 mM Ca and 0.63 mM phenol red (from Pape et al., 1995); the value of the abscissa is 0.65 mM, which represents the concentration of fura-2 that is expected to be comparable to 18.24 mM EGTA in its ability to reduce myoplasmic free $\Delta[\text{Ca}]$. Ringer's solution was used in the central pool in all experiments. In the 12 EGTA-phenol red experiments, the mean values were $f_i = 0.144$ (SEM, 0.004) and $p_1 = 5.25 \text{ \%/ms}$ (SEM, 0.26 \%/ms). Additional information about the EGTA-phenol red experiments is given in the legend of Table II in Pape et al. (1995). Additional information about the fura-2 experiments is given in Pape et al. (1993) under fiber reference 615921 (*open circle*), 616921 (*open square*), 618922 (*open diamond*), and 619921 (*open triangle*).

centrations, might have some pharmacological action that is unrelated to its ability to complex Ca.

The open symbols in Fig. 9 A show the values of f_1 from action-potential experiments in four fibers, plotted as a function of $[\text{fura-2}]_R$. The filled circle shows the mean value of f_1 (\pm SEM) in 12 fibers equilibrated with 20 mM EGTA plus 1.76 mM Ca (from Pape et al., 1995); it is plotted at 0.65 mM "fura-2" on the abscissa, because this concentration of fura-2 is expected to reduce free $\Delta[\text{Ca}]$ to the same extent as equilibration with 20 mM EGTA plus 1.76 mM Ca (see preceding para-

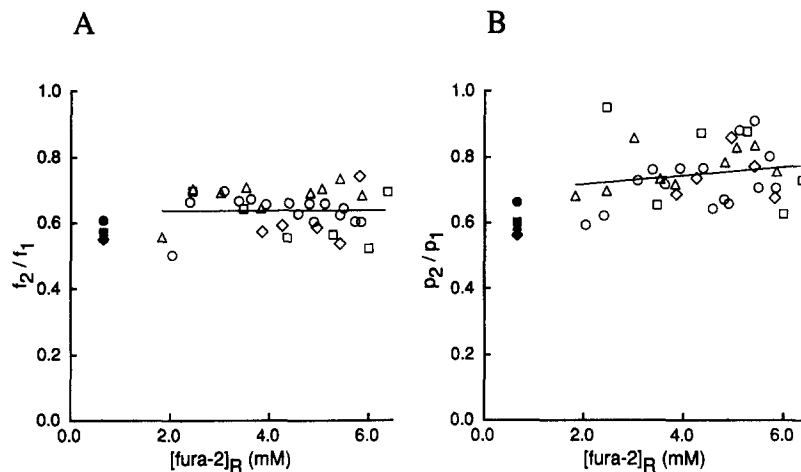


FIGURE 10. Effect of $[\text{fura-2}]_R$ on f_2/f_1 (A) and p_2/p_1 (B) elicited by two action potentials separated by 20 ms. The open symbols show values obtained from the same fibers used in Fig. 9 with the stimulation protocol illustrated in Fig. 2 in Pape et al. (1993). A single action potential was followed by a recovery period of 150 ms and then a 50 Hz train of action potentials. The values of f_1 and p_1 shown in Fig. 9 were taken from the first action potential. The values of f_2/f_1 and p_2/p_1 in this figure were taken from the first two action potentials of the train; the value of $[\text{fura-2}]_R$ represents the value of $[\text{fura-2}]$ before the train. The mean values of the 35 open symbols are 0.638 (SEM, 0.010) for f_2/f_1 and 0.750 (SEM, 0.015) for p_2/p_1 . The filled symbols show the values obtained from the four fibers equilibrated with K-glutamate with 20 mM EGTA plus 1.76 mM Ca and 0.63 mM phenol red that were used for Table III: fiber reference 425911 (*filled circle*), 923911 (*filled square*), 925911 (*filled diamond*), and O10911 (*filled triangle*). In each panel, the continuous straight line was least-squares fitted to the open symbols. The slope of the line is 0.0002 mM^{-1} in A and 0.0131 mM^{-1} in B. According to the test described in the Methods of Pape et al. (1995), neither slope is significantly different from zero. Additional information is given in the text and in the legend of Fig. 9.

graph). The value of the filled circle, 0.144 (SEM, 0.004), is similar to the values of f_1 obtained with ≤ 3 mM fura-2. At concentrations of fura-2 above 4 mM, the value of f_1 progressively decreased. This decrease has been described by Pape et al. (1993), who attributed it to either a reduction in Ca-induced Ca release or a pharmacological effect associated with a large concentration of fura-2.

The open symbols in Fig. 9 B show values of p_1 from the same experiments used

Fig. 9 A. The filled circle shows the mean value of p_1 (\pm SEM) in the 12 fibers equilibrated with 20 mM EGTA plus 1.76 mM Ca (from Pape et al., 1995). Its value, 5.25 %/ms (SEM, 0.26 %/ms), lies at the lower range of the other values in Fig. 9 B obtained with ≤ 3 mM fura-2. The progressive decrease in p_1 above 4 mM fura-2 is similar to that shown for f_1 in A, consistent with the idea that the decrease in f_1 was due to a decrease in p_1 .

In the action-potential experiments in Fig. 9, the values of f_1 (A) and p_1 (B) obtained with ≤ 3 mM fura-2 may be slightly larger than those expected with 0 mM fura-2. According to Pape et al. (1993), 0.5–2 mM fura-2 increases the values of f_1 and p_1 by $\sim 20\%$. In voltage-clamped fibers from the same species of frog (*Rana temporaria*), the same concentration of fura-2 was found to increase the peak rate of SR Ca release by a somewhat larger amount, $\sim 56\%$ (Table I in Jong et al., 1993).

Fig. 10 A shows values of f_2/f_1 that were elicited by two action potentials separated by 20 ms, plotted as a function of $[\text{fura-2}]_R$. The open symbols are from the same fura-2 containing fibers that were used for Fig. 9; their mean value is 0.638 (SEM, 0.010), which is significantly different from unity. The filled symbols are from four other fibers that had been equilibrated with 20 mM EGTA and 1.76 mM Ca and were used for Table III; their mean value, 0.570 (SEM, 0.013), is significantly different from the mean value of the open symbols. The sloping straight line was least-squares fitted to the open symbols. According to the test described in the Methods section of Pape et al. (1995), the value of its slope, 0.0002 mM^{-1} , is not significantly different from zero.

Fig. 10 B is similar to Fig. 10 A except that p_2/p_1 is plotted instead of f_2/f_1 . The mean value of the open symbols, 0.750 (SEM, 0.015), is significantly different from unity and from the mean value of the filled symbols, 0.603 (SEM, 0.021). The slope of the fitted line, 0.0131 mM^{-1} , is not significantly different from zero.

Fig. 11 shows values of the quasi-steady to peak ratio of $d\Delta[\text{Ca}_T]/dt$ obtained in voltage clamp experiments with step depolarizations to 10 mV, plotted as a function of $[\text{fura-2}]_R$. In the four fibers represented by open symbols, $[\text{Ca}]$ transients were first measured with PDAA at $[\text{fura-2}]_R = 0$ mM; the mean value of the ratio data is 0.232 (SEM, 0.016). Then, fura-2 was added to the end-pool solutions and allowed to diffuse into the fiber (Jong et al., 1993). The mean value of the ratio data for $[\text{fura-2}]_R \geq 3.9$ mM, 0.841 (SEM, 0.015), is significantly different from the value for 0 mM $[\text{fura-2}]_R$, 0.232, and from unity. The straight line was least-squares fitted to the open symbols for $[\text{fura-2}]_R \geq 3.9$ mM. Its slope, -0.018 mM^{-1} , is not significantly different from zero.

The cross and x at 0.65 mM "fura-2" show values of the quasi-steady to peak ratio of $d\Delta[\text{Ca}_T]/dt$ obtained from two other fibers that were equilibrated with 20 mM EGTA plus 1.76 mM Ca and studied with the same external solution and voltage step that was used for the fura-2 experiments; the x is from the fiber in Fig. 1 B. The mean value, 0.597 (SEM, 0.060), is significantly different from the values given above for 0 and ≥ 3.9 mM $[\text{fura-2}]_R$.

Figs. 1, 10, and 11 and other results provide information about the ability of different concentrations of Ca buffers to reduce Ca inactivation of Ca release. Two main conclusions follow from these results. Firstly, equilibration with 20 mM EGTA increases the quasi-steady rate of SR Ca release (Fig. 1) and the quasi-steady to peak

ratio of release (Fig. 11) severalfold. The increase in the quasi-steady rate of release is similar to that observed with 2–3 mM fura-2 (Table IIIA in Jong et al., 1993). Since equilibration with 20 mM EGTA is expected to reduce myoplasmic free $[Ca]$ to the same extent as 0.65 mM fura-2, at least for small amounts of SR Ca release, the results with fura-2 and EGTA are consistent with each other. They suggest that the Ca buffering power of 0.65–3 mM fura-2 reduces the effect of Ca inactivation of Ca release severalfold.

Secondly, although large concentrations of fura-2, 2–6 mM in Fig. 10 and 4–8 mM in Fig. 11, are more effective than 20 mM EGTA in reducing Ca inactivation of Ca release, they are unable to completely eliminate it. Thus, in Fig. 10, A and B, and Fig. 11 B, the mean values of the open symbols are all significantly less than

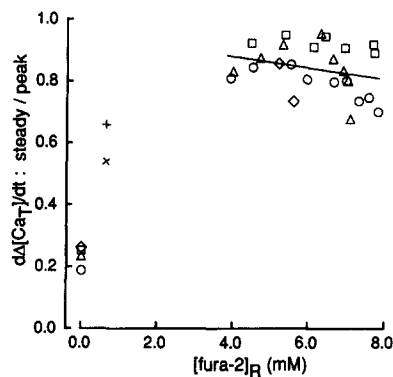


FIGURE 11. The effect of $[fura-2]_R$ on the quasi-steady to peak ratio of $d\Delta[Ca_T]/dt$ during a step depolarization to 10 mV. The TEA-methanesulfonate solution was used in the central pool. The end pool solution was Cs-glutamate with ~ 3 mM PDAA (*open symbols*, $[fura-2]_R = 0$ mM), Cs-glutamate with 20 mM EGTA plus 1.76 mM Ca and 0.63 mM phenol red (*cross* and *x* at $[fura-2]_R = 0.65$ mM), or Cs-glutamate with PDAA and 8 mM fura-2 plus 0–2 mM Ca (*open symbols*, $[fura-2]_R > 3.9$ mM). The mean values were 0.232 (SEM, 0.016) with $[fura-2]_R = 0$ mM, 0.597 (SEM, 0.060) for $[fura-2]_R = 0.65$ mM, and 0.841 (SEM, 0.015)

with $[fura-2]_R > 3.9$ mM. The straight line represents a least-squares fit to the open symbols for $[fura-2]_R > 3.9$ mM; its slope, -0.018 mM^{-1} , is not significantly different from zero. Fiber references: *x*, 314921; *cross* (mean of four measurements), 316921; *diamond*, 325921; *triangle*, 616922; *square*, 617921; *circle*, 618921. Fiber 316921: time after saponin treatment of the end pool segments, 84–114 min; sarcomere spacing, 3.7 μm ; fiber diameter, 121–120 μm ; holding current, -33 to -35 nA; temperature, 14°C; concentration of phenol red at the optical site, 1.174–1.569 mM; estimated pH_R and free $[Ca]_R$, 6.937–6.910 and 0.048–0.055 μM , respectively; $[Ca_{SR}]_R$, 2,483–2,180 μM . Additional information for fiber 314921 is given in the legend of Fig. 1. Additional information for fibers 325921, 616922, 617921, and 618921 is given in Jong et al. (1993).

unity and the slopes of the fitted lines are all not significantly different from zero. The simplest interpretation of these results is that concentrations of fura-2 as large as 6–8 mM are unable to completely eliminate Ca inactivation of Ca release, whether it is elicited by an action potential or by a step depolarization to 10 mV. Another interpretation of these results, however, which cannot be ruled out, is that 6–8 mM fura-2 completely eliminates Ca inactivation of Ca release and that the remaining inactivation is Ca independent.

DISCUSSION

This article describes experiments on Ca inactivation of Ca release in cut muscle fibers activated by either an action potential or a depolarizing voltage pulse. EGTA

(plus phenol red) or fura-2 was added to the end-pool solutions in relatively large concentrations so that SR Ca release could be monitored in a direct fashion. In spite of the ability of EGTA and fura-2 to reduce the amplitudes of the spatially averaged myoplasmic free [Ca] transient and of the local increase in free [Ca] near the SR release sites, substantial amounts of inactivation were still able to develop. Most of our observations concerning this inactivation were obtained from measurements of the rate of SR Ca release, $d\Delta[\text{Ca}_T]/dt$ (corrected for SR Ca depletion), in fibers equilibrated with 20 mM EGTA and depolarized to -20 mV. The main results from these studies are:

(a) During a step depolarization to -20 mV, $d\Delta[\text{Ca}_T]/dt$ reached a peak value within 5–15 ms and then rapidly decayed to a quasi-steady level that was about half the peak value; the time constant of the final decrease of the signal was usually ~ 2 ms at -20 mV (Fig. 4 and text), corresponding to an apparent rate constant of ~ 500 s $^{-1}$. The quasi-steady value of $d\Delta[\text{Ca}_T]/dt$ in fibers equilibrated with 20 mM EGTA was substantially larger than that in fibers with unmodified [Ca] transients: about six times larger if SR Ca release is estimated without consideration of SR Ca pump activity and about four times larger if release is estimated with pump activity (Fig. 1 A and associated text).

(b) Immediately after an action potential or a 10–15 ms prepulse to -20 mV, the peak value of $d\Delta[\text{Ca}_T]/dt$ elicited by a second stimulation, as well as the fractional value of $\Delta[\text{Ca}_T]$, were substantially decreased (Figs. 2 and 3; Tables III and IV). In addition, the time course of the second $d\Delta[\text{Ca}_T]/dt$ signal was changed: the time to half peak of the signal was increased and the initial rising phase was decreased (Fig. 5). The decrease of the rising phase suggests that at least 0.9 of the SR Ca release sites were inactivated by the prepulse (columns 8 and 11 in Table IV). These changes in the time course of $d\Delta[\text{Ca}_T]/dt$ were accompanied by little, if any, change in intramembranous charge movement (Fig. 8).

(c) These effects of a prepulse on the test $d\Delta[\text{Ca}_T]/dt$ signal are removed during a repolarization to -90 mV according to an exponential time course (Figs. 2, 3, and 6). The value of the recovery time constant was ~ 25 ms in the action-potential experiments (columns 5 and 9 in Table III) and ~ 50 ms in the voltage-clamp experiments (columns 4, 7, 10, and 13 in Table IV); these correspond to apparent rate constants of ~ 40 and 20 s $^{-1}$, respectively.

Several Observations Are Consistent with the Idea That the Inactivation Described Above (Results a–c) Is Mainly Caused by Ca

In the experiments reported in this article, all of the measurements of $d\Delta[\text{Ca}_T]/dt$ have been corrected for SR Ca depletion and expressed in terms of fractional rates or fractional amounts of release. As a result, SR Ca depletion, at least in its simplest form, can be ruled out as a cause of the inactivation of Ca release.

Because most of the Ca inside the SR is expected to be bound to calsequestrin, the low affinity Ca buffer that is present inside the terminal cisternae of the SR (MacLennan and Wong, 1971), the possibility arises that the equilibration of Ca and calsequestrin might be slow. If so, the inactivation of Ca release during depolarization might be explained by a decrease in the value of free [Ca] inside the SR, and recovery after release might be explained by an increase in free [Ca] produced

by the dissociation of Ca from calsequestrin. This possibility seems unlikely for two reasons. Firstly, millimolar concentrations of EGTA (or fura-2), which greatly reduce the myoplasmic free [Ca] transient, substantially augment both the peak and quasi-steady values of $d\Delta[\text{Ca}_T]/dt$. Such augmentation is not expected if the decay of $d\Delta[\text{Ca}_T]/dt$ to its quasi-steady level in fibers equilibrated with only 0.1 mM EGTA is due to a decrease of free [Ca] inside the SR; it is readily explained, however, by a reduction in Ca-inactivation of Ca release. Secondly, the reaction between Ca and calsequestrin appears to be rapid, with a relaxation time of <1 ms (Prieto, Donoso, Rodriguez, and Hidalgo, 1994). This rapid rate of equilibration should insure that, during SR Ca release, the value of free [Ca] inside the SR is maintained close to the equilibrium value determined by the concentrations of Ca-free and Ca-bound calsequestrin.

It is also unlikely that changes in intramembranous charge movement underlie the inactivation of Ca release because little change was observed.

Several observations are consistent with the idea that the inhibitory effects on SR Ca release observed in fibers equilibrated with 20 mM EGTA (described above in results *a-c*) are mainly caused by Ca inactivation. Firstly, the reduction in amplitude of the test $d\Delta[\text{Ca}_T]/dt$ signal after a prepulse is similar to that observed by Schneider and Simon (1988) in fibers with unmodified [Ca] transients. These authors provided good evidence that the reduction was caused by Ca inactivation (see text discussion of Fig. 2). Secondly, as mentioned in the preceding paragraph, during a step depolarization, both the peak and quasi-steady levels of the $d\Delta[\text{Ca}_T]/dt$ signal are increased by equilibration with 20 mM EGTA (Fig. 1). The decrease in the $d\Delta[\text{Ca}_T]/dt$ signal from the peak to quasi-steady level that still remains in this condition, however, is qualitatively similar to that observed in fibers with unmodified [Ca] transients (Fig. 1) and attributed to Ca inactivation of Ca release. Thirdly, 2–8 mM fura-2, which is expected to be 3–12 times more effective than 20 mM EGTA in reducing increases in free [Ca], appears to be more effective than 20 mM EGTA in reducing the inactivation of SR Ca release (Figs. 10 and 11); it is not clear, however, whether this effect of fura-2 is due to its ability to buffer Ca or to some other, perhaps pharmacological, action. Fourthly, as is shown in the following two sections, results *a-c* are qualitatively consistent with the model of Ca inactivation of Ca release proposed by Schneider and Simon (1988).

*Interpretation of Results a-c with the Model of Ca Inactivation of Ca Release
Proposed by Schneider and Simon (1988)*

This section describes calculations that were carried out with the model of Ca inactivation of Ca release proposed by Schneider and Simon (1988). Results *a* and *c* were used to estimate the values of three unknown parameters in the model. Calculations were then carried out with these values and compared with the findings listed under result *b*. Since the main purpose of these calculations was to find out whether the Schneider-Simon model could explain, qualitatively, results *a-c*, no attempt was made to reproduce the quantitative features of the experimental traces.

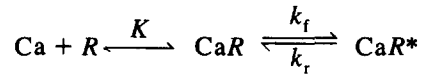
The calculations depend on several simplifying assumptions about the properties of SR Ca channels, which were first proposed by Schneider and Simon (1988). Firstly, the SR Ca channels are assumed to function as a uniform population of a

single type of channel. Secondly, the value of $f(t)$, the fraction of SR Ca channels that are open at time t , is assumed to be determined by an activation process, controlled by a voltage sensor in the transverse tubular membranes, and by an inactivation process, controlled by a receptor that responds to the level of myoplasmic free $[Ca]$. These processes are assumed to operate independently so that $f(t)$ can be represented by the product of an activation function $a(t)$ and an inactivation function $b(t)$,

$$f(t) = a(t) \cdot b(t) . \quad (2)$$

The value of $a(t)$ varies from 0 to 1, with 1 corresponding to full activation. The value of $b(t)$ varies from 0 to 1, with 0 corresponding to full inactivation. $d\Delta[Ca_T]/dt$ (corrected for SR Ca depletion) is assumed to be proportional to $f(t)$.

The third general assumption is that the stoichiometry of Ca binding to the inactivation receptor is 1:1 and that there is only one receptor per channel. The fourth assumption is that this binding obeys the sequential, three-state model proposed by Schneider and Simon (1988)



SCHEME I

R represents an inactivation receptor that is able to equilibrate with free Ca very rapidly to form CaR ; the dissociation constant for the reaction is denoted by K . k_f and k_r represent the forward and reverse rate constants, respectively, for the transition between CaR and CaR^* . The values of K , k_f , and k_r are assumed to be constants; in particular, they are assumed to be independent of membrane potential and of the values of $a(t)$, $b(t)$, and $f(t)$. According to this scheme, an SR Ca channel is able to pass Ca ions if the receptor is in state R or CaR but not if it is in state CaR^* , the inactivated state.

Melzer et al. (1984) and Schneider and Simon (1988) observed that, during a step depolarization, the apparent rate constant for the decrease in $d\Delta[Ca_T]/dt$ from its peak to its quasi-steady level is independent of voltage and of the value of free $[Ca]$, at least at voltages between -40 and 0 mV. Schneider and Simon (1988) introduced Scheme I to explain this observation. If $[Ca] \gg K$, the CaR state is strongly favored over R so that almost all of the receptors are in the CaR or the CaR^* state. Consequently, the apparent rate constant for transitions between the two states approaches its upper limit, $k_f + k_r$, which is independent of $[Ca]$. In contrast, the apparent rate constant for a two-state scheme does not approach an upper limit but continues to increase with increasing $[Ca]$ (see below).

In Scheme I, $b(t)$ represents the fraction of channels that are in either state R or CaR . Changes in $b(t)$ can be calculated from

$$db(t)/dt = -k_f \cdot \frac{[Ca]}{[Ca] + K} \cdot b(t) + k_r \{1 - b(t)\} , \quad (3)$$

in which $[Ca]$ represents the concentration of Ca sensed by the inactivation receptor.

For a particular value of $[Ca]$, k_{app} , the apparent rate constant for transitions between the noninactivated and inactivated states in Eq. 3, is given by

$$k_{app} = k_f \cdot \frac{[Ca]}{[Ca] + K} + k_r, \quad (4)$$

and the steady state value of b is given by

$$b(\infty) = k_r/k_{app}. \quad (5)$$

(In the special case in which $[Ca] \ll K$, the fraction of receptors in the CaR form is much less than that in the R form and $k_{app} \cong (k_f/K) [Ca] + k_r$. Under these conditions, Scheme I is mathematically equivalent to a two-state model in which the forward and reverse rate constants are given by k_f/K and k_r , respectively.)

Eq. 3 can be used to calculate the time course of inactivation of SR Ca release if the value of free $[Ca]$ next to the inactivation receptor is known. During SR Ca release in fibers equilibrated with 20 mM EGTA, local increases in $[Ca]$ are expected to occur within a few hundred nanometers of the SR Ca release sites; these are expected to have an amplitude that varies inversely with distance from the sites and a time course that is approximately the same as that of SR Ca release (Pape et al., 1995). Because the rate of release is expected to be proportional to $f(t)$, the value of $[Ca]$ near the inactivation receptor can be represented by,

$$[Ca] = [Ca]_R + c_1 f(t). \quad (6)$$

$[Ca]_R$ represents the resting value of myoplasmic free $[Ca]$ and c_1 represents a constant whose value depends on the proximity of the inactivation receptor to the release sites. Eq. 6 is only approximately correct because it neglects the effects of changes in the ratio $[CaEGTA]/[EGTA]$ on $[Ca]_R$ (see Eq. A8 in Pape et al., 1995) and of SR Ca depletion on c_1 .

Simon et al. (1991) showed that the value of $[Ca]_R$ in their experiments, carried out on cut fibers equilibrated with an internal solution that contained only 0.1 mM EGTA, was sufficiently small that Ca inactivation of Ca release did not develop to any detectable extent at the holding potential. If the same is true in our experiments on cut fibers equilibrated with 20 mM EGTA, the value of $[Ca]_R$ in Eq. 6 can be neglected and Eqs. 3 and 4 can be written

$$db(t)/dt = k_r - k_{app}b(t) \quad (7)$$

and

$$k_{app} = k_f \cdot \frac{f(t)}{f(t) + K/c_1} + k_r. \quad (8)$$

In the calculations described below, $a(t)$ has been described rather arbitrarily by another variable, $x(t)$, that satisfies a first order differential equation (i.e., a Hodgkin-Huxley variable) and is raised to a power n ,

$$a(t) = x(t)^n . \quad (9)$$

The steady state values of x at -90 mV, the holding potential, and at -20 mV, the standard depolarization, were assumed to be 0 and 1, respectively.

For our calculations, the values of k_r , k_f , and K/c_1 were adjusted to make the time course of $f(t)$ after a voltage step to -20 mV resemble the experimental $d\Delta[\text{Ca}_T]/dt$ signal in fibers equilibrated with 20 mM EGTA (result *a*). Initial estimates of these parameters were made as follows. The value of k_r is expected to be approximately equal to the rate constant of recovery from inactivation (Eq. 8 with $f(t) \cong 0$). Consequently, in our voltage-clamp experiments on fibers equilibrated with 20 mM EGTA, the value of k_r is expected to be $\sim(50 \text{ ms})^{-1} = 20 \text{ s}^{-1}$ (result *c*).

During a step depolarization to -20 or 10 mV, the time constant of the final decrease of the $d\Delta[\text{Ca}_T]/dt$ signal to its quasi-steady level is determined by Eq. 2 from the final time courses of $a(t)$ and $b(t)$. In the absence of EGTA or fura-2, the free $[\text{Ca}]$ transient is sufficiently large that it is reasonable to assume that the value of k_{app} in Eq. 4 is approximately equal to $k_f + k_r$ (Schneider and Simon, 1988). Consequently, according to Eq. 5, $b(\infty) \cong k_r/(k_f + k_r)$.

In a fiber equilibrated with 20 mM EGTA, the value of $b(\infty)$ is increased by a factor of ~ 4 – 6 (result *a*). For the initial estimates of the parameters, a value of six was used for the factor. Since the value of k_r is not expected to change with the addition of EGTA, the sixfold increase in $b(\infty)$ implies a sixfold decrease in k_{app} (Eq. 5). Hence, in a fiber equilibrated with 20 mM EGTA, $k_{\text{app}} \cong (k_f + k_r)/6$. An estimate of this k_{app} can be obtained from the value of the time constant of the final decrease of the $d\Delta[\text{Ca}_T]/dt$ signal with EGTA, ~ 2 ms (result *a*), on the assumption that $a(t) \cong a(\infty)$. This gives $k_{\text{app}} \cong 500 \text{ s}^{-1}$, from which $k_f \cong 3,000 \text{ s}^{-1}$ is obtained. The assumption that $a(t) \cong a(\infty)$ is likely to be more accurate for signals measured in the presence of EGTA than in its absence because the final decrease of the $d\Delta[\text{Ca}_T]/dt$ signal occurs later in time in the presence of EGTA (Fig. 1 *B*), when activation is expected to be increasing less rapidly. With $k_r = 20 \text{ s}^{-1}$ and $k_{\text{app}} = 500 \text{ s}^{-1}$, Eq. 5 gives $b(\infty) = 0.04$. Because $a(\infty)$ is expected to be approximately unity, $f(\infty) \cong 0.04$. According to Eq. 8, these values of k_{app} , k_f , k_r , and $f(\infty)$ correspond to $K/c_1 \cong 0.2$.

Eqs. 2, 7, 8, and 9 were integrated numerically with the initial estimates of the parameters in Eqs. 7 and 8: $k_r = 20 \text{ s}^{-1}$, $K/c_1 = 0.2$, and $k_f = 3,000 \text{ s}^{-1}$. The value of the rate constant for $x(t)$ at -20 mV in Eq. 9 and the value of n were coarsely adjusted so that the theoretical $d\Delta[\text{Ca}_T]/dt$ signal during a prolonged depolarization would roughly resemble the experimental one. The delay in the onset of the experimental $d\Delta[\text{Ca}_T]/dt$ signal required rather large values of n , 20–30. Since the experimental delay includes delays in tubular depolarization as well as delays associated with the activation process itself, it is difficult to attach any mechanistic significance to such a large value of n ; it has been used simply as a computational convenience. The rate constant for x at -90 mV was coarsely adjusted so that the decrease in the theoretical curve after repolarization (not shown) would roughly resemble the experimental one. In calculations with two pulses, the value of $x(t)$ just before each test pulse was reset to 0 to insure that the time course of $a(t)$ was the same during both the prepulse and the test pulse, in agreement with the similarity of the time course of prepulse and test pulse intramembranous charge movement (Fig. 8); this

adjustment was necessitated by the large value of n and the associated slow rate of decay of $x(t)$ after repolarization. The rate constants for x were assumed to be constant at a given potential and independent of Ca.

After these initial calculations were completed, the values of k_r , k_f , and K/c_1 were coarsely adjusted by trial and error to satisfy two conditions: (a) the steady to peak ratio of $f(t)$ during a voltage step should be ~ 0.5 (result a), and (b) the final time constant of the decay of $f(t)$ to its steady level should be ~ 2 ms (result a). The final values that were adopted for the parameters in Eqs. 7 and 8 were $k_r = 15 \text{ s}^{-1}$, $K/c_1 = 0.25$, and $k_f = 2,000 \text{ s}^{-1}$. The time constants for $x(t)$ in Eq. 9 were 3 ms at -20 mV and 40 ms at -90 mV, and the value of n was 25. These parameters give values of 0.568 for the steady to peak ratio of $f(t)$ and 2.13 ms for the final time constant, consistent with conditions a and b.

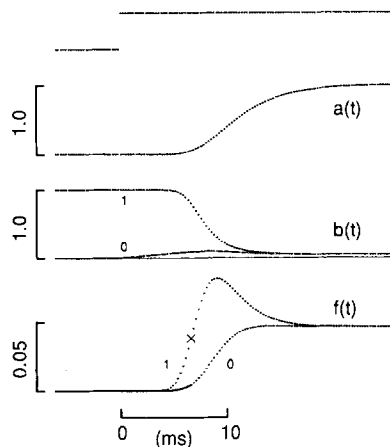


FIGURE 12. Time course of $a(t)$, $b(t)$, and $f(t)$ during a step depolarization. The top trace shows a voltage step to -20 mV. The next trace shows $a(t)$, calculated from Eq. 9. The steady state value of x was 0 at -90 mV (the initial condition) and 1 at -20 mV; the value of the time constant was 3 ms at -20 mV and, in calculations shown in Fig. 13, 40 ms at -90 mV; the value of n was 25. The next two traces show $b(t)$, calculated from Eqs. 7 and 8 with two different initial conditions, $b(0) = 1$ and 0, as indicated; $k_r = 15 \text{ s}^{-1}$, $K/c = 0.25$, and $k_f = 2,000 \text{ s}^{-1}$. The thin continuous line shows the baseline. The bottom two traces show $f(t)$. These were calculated from $a(t)$ and $b(t)$ according to Eq. 2. The $f(t)$ trace calculated with $b(0) = 1$ was scaled to fit the $b(0) = 0$ trace from the beginning of the interval to the half peak of trace 1, indicated by an x ; the scaling constant is 0.103. Additional information is given in the text.

Qualitative Agreement between the Experimental Results and the Predictions of the Schneider-Simon Model

Fig. 12 shows the theoretical time courses of $a(t)$, $b(t)$, and $f(t)$ during a step depolarization to -20 mV. These traces were obtained by numerical integration of Eqs. 2, 7, 8, and 9 with the parameters given in the preceding paragraph (and also in the figure legend).

The first two traces show voltage and $a(t)$, respectively. After depolarization, the increase in $a(t)$ occurs after a marked delay, in agreement with the delay in the experimental $d\Delta[\text{Ca}_T]/dt$ signal. The two $b(t)$ traces, shown below the $a(t)$ trace, were calculated with the initial conditions $b(0) = 0$ and 1, as indicated; although the

value of b should never be $< k_r / (k_f + k_r) = 0.00744$, a value of 0 has been used for purposes of illustration. After very different initial time courses, both traces approach the same final level, 0.0460, which is approximately six times the value of $k_r / (k_f + k_r)$.

The bottom traces in Fig. 12 show $f(t)$, which, as mentioned above, is assumed to be proportional to $d\Delta[\text{Ca}_T]/dt$. The waveform calculated with the initial condition $b(0) = 1$ is similar to that of the $d\Delta[\text{Ca}_T]/dt$ traces obtained from fibers equilibrated with 20 mM EGTA (Fig. 1 B). After depolarization, $f(t)$ increases with a delay and, after 9–10 ms, reaches a peak value of 0.0810. At the time of the peak, the values of $a(t)$ and $b(t)$ are 0.268 and 0.303, respectively, showing that, according to the assumptions in the model, activation is only 27% complete and inactivation is already prominent ($\sim 70\%$ of maximum). Thereafter, $f(t)$ starts to decrease and, because the value of $a(\infty)$ is assumed to be unity, eventually reaches the same final level as $b(t)$, 0.0460, indicating that only 4.6% of the SR Ca channels are open in the steady state. As mentioned at the end of the preceding section, the steady to peak ratio of $f(t)$ is 0.568 and the time constant of the final decay is 2.13 ms.

The other $f(t)$ trace in Fig. 12 was calculated with the initial condition $b(0) = 0$. It has a smaller peak value than the $f(t)$ trace calculated with $b(0) = 1$ and it increases more slowly, because the initial rise of $f(t)$ now depends on the rise of both $a(t)$ and $b(t)$. These differences are similar to those observed experimentally when a prepulse $d\Delta[\text{Ca}_T]/dt$ signal is compared with a test pulse signal in which the effects of Ca inactivation of Ca release are apparent (Fig. 5).

The $f(t)$ trace calculated with the initial condition $b(0) = 1$ was scaled to fit the $b(0) = 0$ trace in the interval from the beginning of the trace to its half peak, marked by an x . The continuous curve at the bottom of Fig. 12 shows the fit, with a scaling factor equal to 0.103.

Although no attempt was made to express $a(t)$ in terms of intramembranous charge movement, it is of interest to compare the value of $a(\text{peak})$, 0.268, with the value of intramembranous charge, Q_{cm} , at the time of the peak. In the experiment illustrated in Fig. 5, Q_{cm} was estimated to be 14.26 nC/ μF at the time of the peak rate of SR Ca release [which is expected to correspond to the peak value of $f(t)$]. At the end of a 250-ms pulse, Q_{cm} was estimated to be 31.25 nC/ μF ; this value, measured for a test potential of -20 mV, is near the maximal value measured at larger depolarizations. The ratio, $14.26/31.25 = 0.456$, represents the fraction of available charge that had moved at the time of the peak rate of SR Ca release. According to Melzer et al. (1986), not all of this charge is able to activate SR Ca channels. In their study of Ca inactivation of Ca release, Schneider and Simon (1988) assumed that 30% of the total available charge must move before activation can occur. If we make the same assumption and also assume that the total available charge is equal to 31.25 nC/ μF , $0.3 \times 31.25 = 9.38$ nC/ μF must be subtracted from the peak and steady state amounts of charge to give the corresponding amounts of activation charge. Accordingly, the fraction of available activation charge that had moved at the time of the peak rate of SR Ca release was $(14.26 - 9.38)/(31.25 - 9.38) = 0.223$, which is consistent with the theoretical value of 0.268 for $a(\text{peak})$ that was obtained in the simulation in Fig. 12.

Fig. 13 shows theoretical traces that were calculated for the pulse protocol used in the experiment in Fig. 5. The top trace shows voltage. The continuous curve in the middle set of traces shows $f(t)$ during the 12-ms prepulse. This curve is the same as the initial part of the $f(t)$ trace labeled 1 in Fig. 12. At the end of the 12-ms prepulse, $f(12 \text{ ms}) = 0.0615$, $a(12 \text{ ms}) = 0.630$, and $b(12 \text{ ms}) = 0.098$.

The dotted traces in the middle of Fig. 13 show $f(t)$ during the test pulse after different periods of repolarization, as indicated (in milliseconds). Two of these $f(t)$ traces are shown at the bottom: the prepulse trace (labeled 1) and the test pulse trace after a 20-ms period of repolarization (labeled 2). The continuous curve shows trace 1 scaled by the constant 0.384, which was obtained from a least-squares fit of trace 1 to trace 2 in the interval from the beginning of the traces to the x .

The middle and bottom traces in Fig. 13 duplicate, at least qualitatively, the main features shown by the experimental traces in Fig. 5: after an inactivating prepulse,

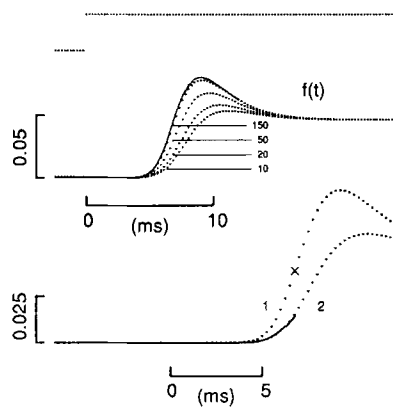


FIGURE 13. Theoretical calculations of the effect of the duration of repolarization on $f(t)$ during a test pulse. Eqs. 2, 7, 8, and 9 were integrated numerically with the pulse protocol that was used for Fig. 5. The traces have been plotted with the same format and time scale that was used in Fig. 5 except that $f(t)$ replaces $d\Delta[\text{Ca}_T]/dt$. The continuous curve at the bottom shows the least-squares fit of trace 1 (prepulse) to trace 2 (test pulse) in the interval from the beginning of the traces to the time to half peak of trace 1, indicated by an x ; the scaling factor is equal to 0.384. Additional information is given in the legend of Fig. 12 and in the text.

the peak amplitude of $f(t)$ during a test pulse is decreased, the time to half peak is increased, and the initial rising phase is decreased (result *b*). The main difference between the theoretical curves in Fig. 13 and the experimental curves in Fig. 5 is that the theoretical curves rise more rapidly than the experimental curves and show less delay in the time to half peak.

The three panels in Fig. 14 are analogous to those in Fig. 6, *A*, *B*, and *D* and are plotted with the same vertical and horizontal scales. Fig. 14 *A* shows the value of p_2/p_1 plotted as a function of the duration of repolarization. The curve shows a fitted decreasing exponential function plus a constant. Its initial value, final value, and time constant—0.587, 0.989, and 51.9 ms, respectively—are similar to the corresponding values obtained in the experiment in Fig. 6 *A*—0.586, 1.002, and 56.4 ms—and to the corresponding mean values in Table IV—0.389, 0.998, and 48.6 ms. These theoretical results are clearly consistent with experimental result *b*.

Fig. 14 *B* shows the value of $\Delta t_{1/2}$ plotted as a function of the duration of repolarization. The initial value of the fitted exponential curve, 1.352 ms, is much smaller than that in Fig. 6 *B*, 4.431 ms, indicating that the experimental effect on $\Delta t_{1/2}$ was more marked than our calculations with Scheme I predict. The final value of the curve in Fig. 14 *B*, 0.075 ms, and the value of the point at 150 ms, 0.057 ms, are also less than the corresponding values in Fig. 6 *B*, 0.593 and 0.557–0.583 ms, respec-

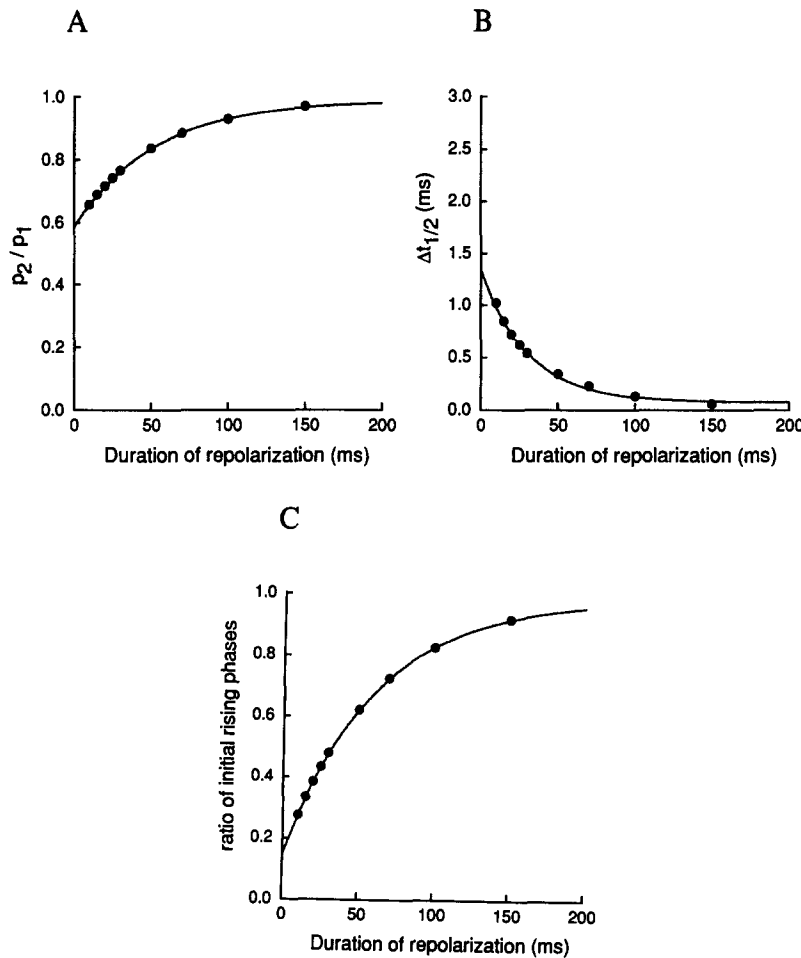


FIGURE 14. Effect of repolarization time on p_2/p_1 (A), $\Delta t_{1/2}$ (B), and the ratio of the initial rising phases (C), from the set of calculations illustrated in Fig. 13. Each continuous curve represents a least-squares fit of a decreasing exponential function plus a constant to the data. In A, the curve has an initial value of 0.587, a final value of 0.989, and a time constant of 51.9 ms. In B, the curve has an initial value of 1.352 ms, a final value of 0.075 ms, and a time constant of 30.3 ms. In C, the curve has an initial value of 0.147, a final value of 0.988, and a time constant of 60.3 ms. Each panel has the same horizontal and vertical axes that were used in the corresponding panel in Fig. 6. Additional information is given in the legends of Figs. 12 and 13 and in the text.

tively. Thus, Scheme I does not explain the large experimental value of $\Delta t_{1/2}$ at 150 ms. The time constant of the curve in Fig. 14 *B*, 30.3 ms, is about half those in Fig. 14 *A* (51.9 ms) and Fig. 14 *C* (60.0 ms), similar to the differences in time constant in Fig. 6 *B* (21.5 ms) and in Fig. 6 *A* (56.4 ms), Fig. 6 *C* (40.7 ms), and Fig. 6 *D* (35.4 ms). These theoretical results are qualitatively consistent with experimental result *b* although, as just mentioned, some quantitative differences exist.

Fig. 14 *C* shows the values of the ratio of the initial rising phases. Since the experimental time course of recovery has both a rapid and slow phase, Fig. 14 *C* should probably be compared with results analyzed according to the procedure in Fig. 6 *D*, which shows the rapid phase of recovery, rather than that in Fig. 6 *C*, which reflects both the rapid and slow phases. The initial and final values of the fitted curve in Fig. 14 *C*, 0.147 and 0.988, are similar to the mean experimental values, 0.126 and 1.084, respectively, given in columns 11 and 12 in Table IV. The value of the time constant of the exponential function in Fig. 14 *C*, 60.3 ms, is also similar to that in Fig. 14 *A*, 51.9 ms (result *c*). These theoretical results are qualitatively consistent with experimental result *b*.

The calculations in Figs. 12–14 were carried out to simulate experimental results obtained from fibers equilibrated with 20 mM EGTA. If the concentration of EGTA is only 0.1 mM, however, as in the experiments used for Fig. 1 *A*, a large increase in free [Ca] can occur throughout the myoplasm. A simple, but rough, approximation of this increase in bulk myoplasmic free [Ca] is given by the integral of $d\Delta[\text{Ca}_T]/dt$ times a scaling factor. Since $d\Delta[\text{Ca}_T]/dt$ is assumed to be proportional to $f(t)$, the increase in [Ca] can be represented by a constant, c_2 , times the integral of $f(t)$, and Eq. 6 can be replaced by

$$[\text{Ca}] = [\text{Ca}]_R + c_1 f(t) + c_2 \int_0^t f(\tau) d\tau. \quad (10)$$

If $[\text{Ca}]_R$ can be ignored (see above), Eq. 8 can be replaced by

$$k_{\text{app}} = k_f \cdot \frac{f(t) + (c_2/c_1) \int_0^t f(\tau) d\tau}{f(t) + (c_2/c_1) \int_0^t f(\tau) d\tau + K/c_1} + k_r. \quad (11)$$

Strictly speaking, the assumption that the increase in bulk myoplasmic free [Ca] is proportional to $d\Delta[\text{Ca}_T]/dt$ implies that the concentration of bound Ca inside the myoplasm is proportional to the concentration of free Ca. Melzer et al. (1984) used this proportionality to describe in a simple fashion the properties of the rapidly equilibrating Ca buffers in myoplasm in fibers equilibrated with only 0.1 mM EGTA. At early times after a strong depolarization, when Ca is binding in a saturating manner to Ca-free troponin and Ca, Mg-free parvalbumin, this approximation

may be overly simple. Nonetheless, as shown by Melzer et al. (1984), it can produce reasonable estimates of SR Ca release and, for this reason, is considered to be a reasonable assumption here, at least during the early phase of SR Ca release. At later times, however, as the value of bulk myoplasmic free [Ca] becomes large and the rapidly equilibrating Ca buffers become saturated with Ca, the value of the proportionality constant is expected to change. Fortunately, at the same time, the progressively increasing value of bulk myoplasmic free [Ca], which is represented by the integral terms in Eq. 11, makes the value of k_{app} approach $k_f + k_r$. As a result, the exact expression that is used to describe bulk myoplasmic free [Ca] becomes less critical.

Fig. 15 shows traces of $f(t)$ calculated from Eqs. 2, 7, 9, and 11 with $c_2/c_1 = 0$ and 2 ms^{-1} , to simulate 20 and 0.1 mM EGTA, respectively. The values of the other parameters were the same as those used for the calculations in Figs. 12–14 except for the value of the time constant for $x(t)$ during the depolarization; it was 2.5 ms, instead of 3 ms, to compensate for the different pulse voltages (10 mV in Figs. 1 and

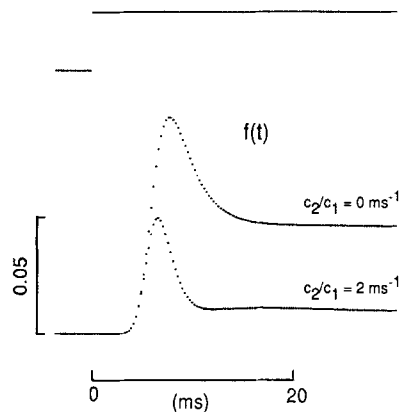


FIGURE 15. Theoretical calculations of the effect of 20 mM EGTA on $f(t)$ during a step depolarization to 10 mV, to compare with the experimental traces in Fig. 1. The top trace shows voltage. The two bottom traces show $f(t)$, calculated as described in the legend of Fig. 12 except that Eq. 11 instead of Eq. 8 was used for k_{app} ; $c_2/c_1 = 0$ and 2 ms^{-1} (as indicated) were used to simulate the effects of 20 and 0.1 mM EGTA, respectively. The other parameters were the same as those given in the legend of Fig. 12 except that the time constant for $x(t)$ was 2.5 ms instead of 3 ms to allow for the more positive potential, 10 mV instead of -20 mV . Additional information is given in the text.

15, and -20 mV in Figs. 5 and 12–14). With $c_2/c_1 = 0 \text{ ms}^{-1}$, the peak and steady state values of $f(t)$ are 0.0928 and 0.0460, respectively. When the value of c_2/c_1 is increased to 2 ms^{-1} , the peak value of $f(t)$ is decreased to 0.0494, the value at the end of the trace (30 ms) is decreased to 0.00986, and the value as $t \rightarrow \infty$ is equal to $k_r/(k_f + k_r) = 0.00744$. These decreases in $f(t)$ are expected from the increase in c_2/c_1 , which allows an increase in bulk myoplasmic free [Ca] to be added to the value of local [Ca] next to the inactivation receptor.

The comparison shown in Fig. 15 is qualitatively similar to that shown in the middle panel of Fig. 1 B. The effect of reducing the value of c_2/c_1 from 2 to 0 ms^{-1} was to increase the peak and quasi-steady (30 ms) values of $f(t)$ by factors of $0.0928/0.0494 = 1.9$ and $0.0460/0.00986 = 4.7$, respectively. The corresponding experimental factors were similar. The factors for the increases in the peak and quasi-steady values were $2.36/1.09 = 2.2$ and $1.37/0.36 = 3.8$, respectively (if the rate of

binding and translocation of Ca by the SR Ca pump is added to $d\Delta[\text{Ca}_T]/dt$ for the estimate of the rate of SR Ca release) and $2.36/0.96 = 2.5$ and $1.37/0.23 = 6.0$, respectively (if it is not). In assessing the significance of this comparison, it is important to remember that the estimation of the rate of SR Ca release with 0.1 mM EGTA is subject to uncertainties, as described in the text discussion of Fig. 1 A, and that the third term on the right-hand side of Eq. 10 represents a rough approximation of bulk myoplasmic free [Ca] in the presence of only 0.1 mM EGTA.

The final time constants of the decay of the $d\Delta[\text{Ca}_T]/dt$ signals in Fig. 15 are 2.23 ms for $c_2/c_1 = 0$ and 0.91 ms for $c_2/c_1 = 2 \text{ ms}^{-1}$. The corresponding mean values from the experiments represented in Fig. 1 were 4.93 and 2.66 ms, respectively. Thus, although the calculations simulate the ability of EGTA to increase the value of the time constant, the actual theoretical values of the time constants are smaller, by a factor of 2–3, than the experimental values. The main reason for this difference relates to an experimental difference between the results obtained in November, 1991 and those obtained in March–June, 1992. The parameters for the calculations in Figs. 12–15 were chosen to match the results in Figs. 5–6 and Table IV. These experiments were carried out in November, 1991 on fibers equilibrated with 20 mM EGTA and studied with the TEA-gluconate solution in the central pool. The mean value of the final time constant was 2.41 ms at -20 mV . On the other hand, the effect of EGTA on the $d\Delta[\text{Ca}_T]/dt$ signal (Fig. 1) was studied in March and June, 1992, with TEA-methanesulfonate in the central pool. In fibers equilibrated with 20 mM EGTA, the mean value of the final time constant was 4.93 ms at 10 mV.

The main conclusion from these calculations is that there is reasonable qualitative agreement between the principal features of the theoretical traces in Figs. 13 and 15 and of the experimental traces in Figs. 5 and 1, respectively. Similarly, the results illustrated in Fig. 14 are qualitatively similar to those in Fig. 6. The main experimental result that is not qualitatively consistent with Scheme 1 is the presence of a small delay in the time to half peak of the test $d\Delta[\text{Ca}_T]/dt$ signal after a 100–150 ms period of repolarization (Figs. 5 and 8 B). This delay, which is not accompanied by a change in intramembranous charge movement (Fig. 8 B), is responsible for the nonzero value of $\Delta t_{1/2}$ that was observed after long periods of recovery (Fig. 6 B) and for the failure of the final value of the ratio of the rising phases to approach unity after long periods of recovery (Fig. 6 C and column 9 in Table IV). Thus, a brief prepulse appears to elicit some change in the kinetics of opening of SR Ca channels that requires a long time ($>150 \text{ ms}$) to recover. Although the cause of this long lasting effect on kinetics has not been determined, possibilities that should be considered include the reduction in SR Ca content or the small increase in resting free [Ca] produced by SR Ca release during the prepulse.

In spite of the success of the Schneider-Simon model in providing a qualitative description of our experimental results, two quantitative discrepancies remain. As mentioned above, the theoretical curves of $f(t)$ in Fig. 13 rise more rapidly than the experimental curves in Fig. 5 and the theoretical increase in $\Delta t_{1/2}$ after a brief period of repolarization (Fig. 14 B) is less marked than the observed increase (Fig. 6 B). The presence of such discrepancies should not be considered surprising in view of the simplicity of the assumptions that have been used for the theoretical model.

For example, the Hodgkin-Huxley activation function for $a(t)$ (Eq. 9) was used as a computational convenience and the power n was selected to reproduce the delay in charging the transverse tubular system as well as the delay in the activation process itself. The resemblance between the theoretical and experimental results might have been improved by the use of different models for the estimation of these two delays, perhaps a cable model for charging the tubular system and a charge movement model for activation. The quantitative discrepancies might also have been reduced by modification of the Schneider-Simon model of inactivation for $b(t)$ (Scheme I). For example, Ca inactivation of a channel might require the binding of more than one Ca ion, as indicated by the experimental results of Simon et al. (1991). If so, the binding sites could be at different myoplasmic locations that sense different increases in free [Ca] during release. It is also possible that Ca inactivation of Ca release is produced more efficiently by Ca flux through the same channel than by Ca flux through neighboring channels (see, for example, pages 364–366 in Jong et al., 1993; and Pizzarró and Ríos, 1994). In this case, the same $b(t)$ function would not apply to every SR release site and the fundamental assumption that $b(t)$ acts independently of $a(t)$ would not be expected to hold. Another more hypothetical possibility is that K , k_f , or k_r may not be constant but may depend on voltage or the value of $a(t)$ or $b(t)$. We have not attempted to explore these or many other possibilities because of the lack of experimental information to guide us. Rather, the calculations illustrated in Figs. 12–15 represent a first attempt to reproduce the main qualitative features of Ca inactivation of Ca release observed in our experiments.

Ca-induced Ca Release

In fibers equilibrated with 20 mM EGTA, local increases in myoplasmic free [Ca] during SR Ca release are expected to occur only within a few hundred nanometers of the release sites (Appendices B and D in Pape et al., 1995). As a result, any modulation of SR Ca release by Ca would be expected to be caused by changes in Ca concentration within this region. Such modulation includes Ca-induced Ca release (Endo, Tanaka, and Ebashi, 1968; Ford and Podolsky, 1968; Fabiato, 1984) as well as Ca inactivation of Ca release.

The results in Fig. 9 (see also Pape et al., 1993) show that, after an action potential, both the amount and the rate of SR Ca release are substantially smaller with >4 mM fura-2 than with 2–4 mM fura-2 or 20 mM EGTA. Similar reductions in the rate of Ca release are produced by >4 mM fura-2 during step depolarizations to 10 mV (Jong et al., 1993). If the effects of >4 mM fura-2 are due to the Ca buffering action of fura-2 and not to some other (perhaps pharmacological) effect, they would be consistent with a reduction in Ca-induced Ca release. It is therefore of interest to compare the distance between adjacent SR Ca channels with the distance that a Ca ion is expected to diffuse before it is captured by EGTA or fura-2.

Franzini-Armstrong (1975) and Block, Imagawa, Campbell, and Franzini-Armstrong (1988) have reported that the distance between adjacent “foot” structures, which appear to contain the SR Ca channels (Inui, Saito, and Fleischer, 1987; Lai, Erickson, Rousseau, Liu, and Meissner, 1988), is ~ 30 nm.

Neher (1986) has derived an expression for λ_{Ca} , the characteristic distance that a Ca ion is expected to diffuse before being captured by a Ca buffer. This expression is repeated as Eq. B14 in Pape et al. (1995). In fibers equilibrated with 20 mM EGTA and 1.76 mM Ca, λ_{Ca} is estimated to be 81 nm (Appendix B in Pape et al., 1995). This estimate is based on a value of 3.0×10^{-6} cm²/s for the diffusion coefficient of Ca, D_{Ca} , and a value of 45.6×10^3 s⁻¹ for $k_1[EGTA]_R$ (estimated from direct measurements with PDAA of the spatially averaged $\Delta[Ca]$ signal in the presence of EGTA); if the value of $[EGTA]_R$ at the optical site is the same as that in the end-pool solutions, 18.24 mM, the apparent association rate constant of Ca and EGTA is 2.5×10^6 M⁻¹s⁻¹. The value of λ_{Ca} in the presence of fura-2 can be estimated in a similar way, with a value of 0.7×10^8 M⁻¹s⁻¹ for the apparent association rate constant of Ca and fura-2 (the value measured with 2 mM fura-2, Pape et al., 1993). Values of 46, 33, 27, and 23 nm are obtained for 2, 4, 6, and 8 mM fura-2, respectively. According to the results in Fig. 9 (and in Jong et al., 1993), the inhibitory effects of fura-2 do not become apparent until the value of λ_{Ca} is reduced to ~ 30 nm, which coincides with the distance between adjacent SR Ca channels.

This correlation may be relevant to some of the ideas proposed by Ríos and Pizarró (1988), based on the structural studies of Block et al. (1988) on toadfish swim-bladder muscle. Block et al. (1988) found that the density of tetrads in the transverse tubular membrane, presumed to be composed of dihydropyridine receptors (DHPR), is half that of the "foot" structures (ryanodine receptors) associated with the adjacent SR membranes. Since the DHPR's are probably the voltage sensors for excitation-contraction coupling (Ríos and Brum, 1987; Tanabe, Beam, Powell, and Numa, 1988) and the foot structures are the SR Ca channels (see above), it is plausible to suppose that half of the SR Ca channels are gated by the voltage across the transverse tubular membranes and that the other half are not. (As far as we are aware, information similar to that obtained by Block et al., 1988, from toadfish muscle has not been obtained from amphibian muscle.)

With these ideas in mind, Ríos and Pizarró (1988) introduced the speculation that the non-voltage-gated channels are Ca-gated and that they are opened by Ca ions that are released into the myoplasm by neighboring voltage-gated channels. If correct, it is reasonable to suppose that, once the concentration of fura-2 exceeds 4 mM and the value of λ_{Ca} becomes < 33 nm, fura-2 would be able to complex a substantial fraction of the Ca ions released from voltage-gated channels before they could diffuse to and activate adjacent Ca-gated channels. The decline in f_1 and p_1 observed with > 4 mM fura-2 in Fig. 9 may be consistent with this mechanism. On the other hand, it seems prudent to also keep in mind the possibility that large concentrations of fura-2, > 4 mM, might have an inhibitory action on SR Ca release that is unrelated to the ability of fura-2 to bind Ca.

The Voltage-gated SR Ca Channels Appear to Be Susceptible to Ca Inactivation

In their speculation about voltage-gated and Ca-gated channels, Ríos and Pizarró (1988) proposed that only the Ca-gated channels, and not the voltage-gated channels, are susceptible to Ca inactivation of Ca release. According to their idea, after depolarization, the voltage-gated channels open first and remain open for the duration of the depolarization. Ca ions move through these channels into the myo-

plasm and open neighboring Ca-gated channels. The Ca-gated channels eventually close, however, because of Ca inactivation of Ca release. As a result, only the voltage-gated channels remain open at the end of a long lasting depolarization.

If the inactivation of SR Ca release that is able to develop in the presence of 6–8 mM fura-2 (Figs. 10 and 11) is Ca dependent, our results suggest that the extent of Ca inactivation varied little, if at all, when the concentration of fura-2 was increased from 4 to 6 mM (Fig. 10) or from 4 to 8 mM (Fig. 11). This insensitivity of Ca inactivation of Ca release to fura-2 concentration stands in marked contrast to the progressive reductions in f_i and p_i that were observed in Fig. 9 when the concentration of fura-2 was increased from 4 to 6 mM. If these reductions in f_i and p_i are due to a decrease in the number of Ca-gated channels that are able to open because of complexation of messenger Ca by fura-2 (see preceding section), it would appear that Ca inactivation of Ca release must affect voltage-gated as well as Ca-gated channels.

Additional support for this idea can be obtained from the results in Figs. 5 and 6, obtained from fibers equilibrated with 20 mM EGTA. In the middle traces in Fig. 5, the curves labeled 150 and 10 show $d\Delta[Ca_T]/dt$ signals that were elicited by a test pulse after the fiber had been repolarized by 150 and 10 ms, respectively. In the 150-ms trace, the rapidly recovering component of Ca inactivation of Ca release is expected to have been essentially in the resting state whereas, in the 10-ms trace, it should have been mainly inactivated. (Both signals, however, are expected to have been delayed by ~ 0.5 ms due to the presence of the slowly recovering component of inactivation.)

If, in this experiment, recovery of the rapidly recovering component of Ca inactivation of Ca release followed the exponential time course shown in Fig. 6 D, it is possible to estimate the $d\Delta[Ca_T]/dt$ signal that would have been observed if no recovery had occurred from the inactivation produced by the prepulse. Let $T(d)$ denote the test $d\Delta[Ca_T]/dt$ signal elicited after a period of repolarization of duration d . According to Eq. 1 with the substitution of $T(150 \text{ ms})$ for $T(\infty)$,

$$T(d) = \exp(-d/\tau) \cdot T(0 \text{ ms}) + (1 - \exp(-d/\tau)) \cdot T(150 \text{ ms}). \quad (12)$$

Eq. 12 can be rearranged to give

$$T(0 \text{ ms}) = \exp(d/\tau) \cdot T(d) + (1 - \exp(d/\tau)) \cdot T(150 \text{ ms}). \quad (13)$$

The top trace in Fig. 16 shows the voltage step from Fig. 5. The bottom traces show the $T(150 \text{ ms})$ and $T(0 \text{ ms})$ signals, as indicated. $T(150 \text{ ms})$ is the same as the trace labeled 150 in Fig. 5. $T(0 \text{ ms})$ was calculated from Eq. 13 with the traces labeled 150 and 10 in Fig. 5; for the calculation, $d = 10 \text{ ms}$ and $t = 35.4 \text{ ms}$ (the value of the time constant of the exponential function in Fig. 6 D). The $T(150 \text{ ms})$ and $T(0 \text{ ms})$ traces show $d\Delta[Ca_T]/dt$ with the initial conditions of almost no Ca inactivation of Ca release and almost complete inactivation, respectively. They provide approximate estimates of $y_R(t)$ and $y_I(t)$, respectively, in Eq. 1.

In terms of the speculation of Ríos and Pizarró (1988), $T(150 \text{ ms})$ represents the movement of Ca through both the voltage-gated and Ca-gated channels whereas $T(0 \text{ ms})$ represents Ca movement primarily through voltage-gated channels, be-

cause they are assumed to not inactivate. Because the initial time course of $T(0 \text{ ms})$ is markedly delayed with respect to that of $T(150 \text{ ms})$, the voltage-gated channels appear to open after the Ca-gated channels. This does not agree with the idea that Ca from the voltage-gated channels causes the initial opening of the Ca-gated channels. The results in Fig. 16, then, provide strong evidence for the idea that the SR Ca channels that open first, and are presumably gated by voltage, are susceptible to Ca inactivation of Ca release.

Although our experiments do not resolve the question of how the non-voltage-gated channels (if any) open, it seems unlikely that they are initially opened by Ca from the voltage-gated channels unless the voltage-gated channels are susceptible to Ca inactivation of Ca release. In fact, our results would clearly be consistent with a scheme in which each voltage-gated channel would be susceptible to Ca inactivation

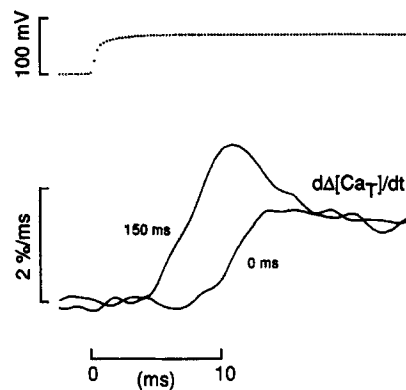


FIGURE 16. The effect of Ca inactivation of Ca release on the time course of the rate of SR Ca release, from the two pulse experiment illustrated in Fig. 5. The top trace shows voltage. The bottom superimposed traces show two $d\Delta[\text{Ca}_T]/dt$, or $T(d)$, signals elicited by the test pulse after periods of repolarization, d , of 150 and 0 ms, as indicated. The trace labeled 150 ms is from Fig. 5. The trace labeled 0 ms was estimated from Eq. 13; it is equal to the 10 ms trace in Fig. 5 scaled by the factor $\exp(10/35.4) = 1.326$ plus the 150 ms trace scaled by the factor $1 - \exp(10/35.4) = -0.326$. See text for additional information.

tion of Ca release and its adjacent non-voltage-gated channels (if any) would function as slaves to it, perhaps with Ca as the gating messenger. In this case, a single voltage-gated channel and its adjacent non-voltage-gated channels would form a collection of channels that function as a singly gated unit. Our results would also be consistent with the simpler scheme in which each voltage sensor in the transverse tubular membranes gates a single SR Ca channel and all of the channels behave as a homogeneous population. In either case, in this article and in Pape et al. (1995), a single SR channel or a cluster of channels that function as a singly gated unit is called a release site. As mentioned above and discussed in the next section, it is possible that far fewer than half of the SR Ca channels may actually be open at the same time after either action-potential or voltage-clamp stimulation. This inference along with estimates of the single-channel current of a ryanodine receptor Ca channel raises the possibility, as pointed out by Block et al. (1988), that the Ca channels

associated with foot structures that are not directly associated with DHPR's are "silent", i.e., do not function as Ca release channels.

*Implications of the Idea That Only a Small Fraction of SR Ca Channels
Can Open at the Same Time*

As mentioned above, two observations support the idea that, after a strong depolarization of a fiber equilibrated with 20 mM EGTA, Ca inactivation of Ca release is sufficiently strong to eventually affect most of the SR Ca channels. The first observation is the marked decrease in the initial rising phase of the $d\Delta[\text{Ca}_T]/dt$ signal that occurs during a test pulse that is applied shortly after a prepulse (Fig. 5 and Table IV). For example, the mean values of columns 8 and 11 in Table IV (0.093 and 0.126) suggest that at least 0.9 of the channels are inactivated immediately after a 10–15-ms prepulse to -20 mV.

The second observation is based on the markedly different values of two rate constants: the rate constant of the final decrease of the $d\Delta[\text{Ca}_T]/dt$ signal to its quasi-steady level, $\sim 500 \text{ s}^{-1}$ during a voltage step to -20 mV, and the rate constant for recovery from inactivation during repolarization, $\sim 20 \text{ s}^{-1}$. If $a(t) \cong a(\infty)$ during the final decrease of the $d\Delta[\text{Ca}_T]/dt$ signal, Scheme I with Eqs. 4 and 5 gives $k_r \cong 20 \text{ s}^{-1}$, $k_{app} \sim 500 \text{ s}^{-1}$, and $b(\infty) = k_r/k_{app} \cong 20/500 = 0.04$. Thus, within the framework of the assumptions, 96% of the activated SR Ca channels are expected to be inactivated after a prolonged depolarization to -20 mV. This expectation relies on the assumption that the value of k_r is constant and, in particular, that it has the same value during a depolarization that it has during a recovery period at -90 mV.

(Note: Schneider and Simon (1988) obtained different values for k_r , k_{app} , and k_r/k_{app} in their experiments carried out on fibers with unmodified [Ca] transients: k_r ($1/\tau_{rec}$ in their nomenclature) = 11 s^{-1} and k_{app} ($1/\tau_{dec}$ in their nomenclature) = 31 s^{-1} , which gives $k_r/k_{app} = 0.35$, an order of magnitude larger than our estimate. Because their experiments were carried out at a lower temperature than ours ($6\text{--}10^\circ\text{C}$ rather than 14°C), and since they consider their value of k_r to be a lower limit because free [Ca] was still decreasing during the first part of their recovery period, our value of $\sim 20 \text{ s}^{-1}$ for k_r is in reasonable agreement with their value of 11 s^{-1} . The main difference, then, between our results and theirs is in the value of k_{app} . The difference is not due to our equilibration of fibers with 20 mM EGTA because fibers with unmodified [Ca] transients, and studied in this laboratory under conditions that were similar to those used for fibers equilibrated with 20 mM EGTA, also gave large values for k_{app} : on average, $(2.66 \text{ ms})^{-1} = 376 \text{ s}^{-1}$ in fibers from *Rana temporaria* and $(1.58)^{-1} = 633 \text{ s}^{-1}$ in fibers from *Rana pipiens* (see text associated with Fig. 1). We have no satisfactory explanation for this marked difference in the values of k_{app} .)

If only 4–5% of the SR Ca channels are open during the quasi-steady level of release, only about twice this amount, 8–10%, are expected to be open at the time of the peak rate of release (result *a*). In a similar series of experiments carried out on fibers equilibrated with 20 mM EGTA, Pape et al. (1995) found that the peak rate of SR Ca release during a strong depolarization was about half of that observed after an action potential; thus, $\sim 16\text{--}20\%$ of the SR Ca channels are expected to be open at the time of the peak rate of Ca release after an action potential in fibers

equilibrated with 20 mM EGTA. One of the explanations suggested for this difference is that the regenerative Na spike in the transverse tubules in the action-potential experiments may allow activation of SR Ca release to be synchronized throughout the cross section of a fiber so that the peak rate of release occurs nearly simultaneously throughout the fiber. This explanation seems attractive in view of the large amount of inactivation that appears to develop after an action potential and the rapid rate of its development, as measured during voltage-clamp experiments.

According to these ideas, it appears that only a small fraction of the SR Ca channels can actually be made to open at the same time by either action-potential or voltage-clamp depolarization. Furthermore, from the simplest considerations, once a channel is activated, it would be expected to remain open for only a brief period of time, on average ~ 2 ms at -20 mV in our EGTA voltage-clamp experiments (given by the value of $[k_{\text{app}} - k_r]^{-1}$). The channel would then close and remain closed for an average period of time of ~ 50 ms (given by the value of k_r^{-1}) before opening again.

An important question to consider is whether such small values of the mean open probability of SR channels are consistent with other measurements. For example, the rate of SR Ca release is determined by the concentration of SR Ca channels (expressed in terms of the myoplasmic solution), their mean open probability, and the single-channel Ca current. In the experiment in Fig. 1 *B*, for example, the peak rate of SR Ca release was $74 \mu\text{M}/\text{ms}$. Pape, Konishi, and Baylor (1992) estimated the concentration of SR Ca channels to be $0.27 \mu\text{M}$, from the concentration of foot structures (Franzini-Armstrong, 1975) on the assumption of a 1:1 stoichiometry. If all of the channels were open (i.e., the mean open probability were one) and the rate of release were $74 \mu\text{M}/\text{ms}$, the flux through each channel would be $\sim 3 \times 10^5$ Ca ions/s, corresponding to a single-channel current of ~ 0.1 pA. On the other hand, if a release rate of $74 \mu\text{M}/\text{ms}$ were supported by only 10% of the channels being open, the single channel current would need to be ~ 1 pA.

Although the flux through a single SR Ca channel has not been measured inside a frog cut muscle fiber, it has been measured in bilayers that contain either native channels (Smith, Coronado, and Meissner, 1986) or channels from purified ryanodine receptor protein (Smith, Imagawa, Ma, Fill, Campbell, and Coronado, 1988) from rabbit skeletal muscle. With 53 mM Ca on the side of the bilayer that corresponds to the lumen of the SR, the single-channel current is ~ 3 pA at 0 mV, 20–22°C. As far as we are aware, currents in single channels from skeletal muscle have not been measured with concentrations of Ca as low as 1–2 mM, the estimated free concentration inside the SR (Hasselbach and Oetliker, 1983). There is considerable evidence, however, that the single-channel current is not directly proportional to free [Ca] between 1–2 and 53 mM. Smith et al. (1988) studied single channels in bilayers with the same concentration of Ca on both sides of the membrane. They found that the relation between conductance at 0 mV and [Ca] could be fitted by a 1:1 binding isotherm with $K_m = 3$ mM. If the same binding isotherm is used to describe the relation between single-channel currents at 0 mV (the likely value of SR membrane potential, Somlyo, Shuman, and Somlyo, 1977) and millimolar free [Ca] on the luminal side of the membrane only, a single-channel current of 3 pA with 53 mM Ca would correspond to 0.79–1.26 pA with 1–2 mM Ca.

Tinker and Williams (1992) and Tinker, Lindsay, and Williams (1992) have carried out an extensive analysis of the permeability properties of purified ryanodine receptor channels isolated from sheep cardiac muscle. From their results, Tinker, Lindsay, and Williams (1993) estimate a value of 2 pA for the single-channel current at 0 mV and 21°C with 2.5 mM Ca on the luminal side of the membrane only.

Based on these results obtained with SR Ca channels in bilayers, a value 1–2 pA for the current through a single SR Ca channel inside a frog cut muscle fiber appears reasonable. These values are clearly consistent with the idea that only a small fraction of SR Ca channels may actually be open at the same time after either an action potential or during a voltage step to positive potentials.

Role of Ca Inactivation of Ca Release during an Action Potential or Brief Voltage Pulse

Although a good case can be made for the idea that most of the SR Ca channels are inactivated by an action potential or a brief depolarization, the main experimental evidence for this idea is provided by measurements of SR Ca release that were elicited by a second stimulation. As a result, it is difficult to determine exactly how much inactivation developed during the first period of depolarization and how much developed during the first few milliseconds after repolarization. Since Ca inactivation of Ca release appears to be able to develop rapidly during depolarization, even in fibers equilibrated with 20 mM EGTA, it is conceivable that inactivation is also able to develop rapidly after repolarization. The importance of this inactivation could be marked if the values of K , k_f , and k_r in Scheme I were not constant but depended on voltage or some other parameter that changes with voltage. For example, if the value of k_r were much larger during a depolarization than during a repolarization to -90 mV, Ca inactivation might develop to a relatively small extent during depolarization and then develop to a large extent after repolarization. If this were the case, the turn off of SR Ca release after repolarization following an action potential or brief voltage pulse could depend strongly on both voltage-dependent deactivation and Ca-dependent inactivation.

We thank the staff of the Biomedical Instrumentation Laboratory of the Yale Department of Cellular and Molecular Physiology for help with the design and construction of equipment. We also thank Dr. Stephen Hollingworth for reading the manuscript and providing useful criticism.

This work was supported by U.S. Public Health Service grants AM-37643 (W. K. Chandler) and NS-17620 (S. M. Baylor).

Original version received 31 March 1994 and accepted version received 17 March 1995.

REFERENCES

- Baylor, S. M., W. K. Chandler, and M. W. Marshall. 1983. Sarcoplasmic reticulum calcium release in frog skeletal muscle fibres estimated from arsenazo III calcium transients. *Journal of Physiology*. 344: 625–666.
- Baylor, S. M., and S. Hollingworth. 1988. Fura-2 calcium transients in frog skeletal muscle fibres. *Journal of Physiology*. 403:151–192.
- Block, B. A., T. Imagawa, K. P. Campbell, and C. Franzini-Armstrong. 1988. Structural evidence for direct interaction between the molecular components of the transverse tubule/sarcoplasmic retic-

- ulum junction in skeletal muscle. *Journal of Cell Biology*. 107:2587–2600.
- Chandler, W. K., and C. S. Hui. 1990. Membrane capacitance in frog cut twitch fibers mounted in a double Vaseline-gap chamber. *Journal of General Physiology*. 96:225–256.
- Endo, M., M. Tanaka, and S. Ebashi. 1968. Release of calcium from sarcoplasmic reticulum in skinned fibers of the frog. *Proceedings of the International Congress of Physiological Sciences*. 7:126. (Abstr.)
- Fabiato, A. 1984. Dependence of the Ca^{2+} -induced release from the sarcoplasmic reticulum of skinned skeletal muscle fibres from the frog semitendinosus on the rate of change of free Ca^{2+} concentration at the outer surface of the sarcoplasmic reticulum. *Journal of Physiology*. 353:56P. (Abstr.)
- Fernandez-Belda, F., M. Kurzmack, and G. Inesi. 1984. A comparative study of calcium transients by isotopic tracer, metallochromic indicator, and intrinsic fluorescence in sarcoplasmic reticulum ATPase. *Journal of Biological Chemistry*. 259:9687–9698.
- Ford, L. E., and R. J. Podolsky. 1968. Force development and calcium movements in skinned muscle fibers. *Federation Proceedings*. 27:375. (Abstr.)
- Franzini-Armstrong, C. 1975. Membrane particles and transmission at the triad. *Federation Proceedings*. 34:1382–1389.
- Gillis, J. M., D. Thomason, J. Lefevre, and R. H. Kretsinger. 1982. Parvalbumins and muscle relaxation: a computer simulation study. *Journal of Muscle Research and Cell Motility*. 3:377–398.
- Hasselbach, W., and H. Oetliker. 1983. Energetics and electrogenicity of the sarcoplasmic reticulum calcium pump. *Annual Review of Physiology*. 45:325–339.
- Hille, B., and D. T. Campbell. 1976. An improved Vaseline gap voltage clamp for skeletal muscle fibers. *Journal of General Physiology*. 67:265–293.
- Hirota, A., W. K. Chandler, P. L. Southwick, and A. S. Waggoner. 1989. Calcium signals recorded from two new purpurate indicators inside frog cut twitch fibers. *Journal of General Physiology*. 94:597–631.
- Hui, C. S., and W. K. Chandler. 1990. Intramembranous charge movement in frog cut twitch fibers mounted in a double Vaseline-gap chamber. *Journal of General Physiology*. 96:257–297.
- Hui, C. S., and W. K. Chandler. 1991. Q_B and Q_T components of intramembranous charge movement in frog cut twitch fibers. *Journal of General Physiology*. 98:429–464.
- Inui, M., A. Saito, and S. Fleischer. 1987. Purification of the ryanodine receptor and identity with feet structures of junctional terminal cisternae of sarcoplasmic reticulum from fast skeletal muscle. *Journal of Biological Chemistry*. 262:1740–1747.
- Irving, M., J. Maylie, N. L. Sizto, and W. K. Chandler. 1987. Passive electrical and intrinsic optical properties of cut frog twitch fibers. *Journal of General Physiology*. 89:1–40.
- Jong, D.-S., P. C. Pape, W. K. Chandler, and S. M. Baylor. 1993. Reduction of calcium inactivation of sarcoplasmic reticulum calcium release in voltage-clamped cut twitch fibers with fura-2. *Journal of General Physiology*. 102:333–370.
- Jong, D.-S., P. C. Pape, S. M. Baylor, and W. K. Chandler. 1994. Two effects of a voltage prepulse on sarcoplasmic reticulum (SR) calcium release in frog cut muscle fibers. *Biophysical Journal*. 66:A340. (Abstr.)
- Konishi, M. and S. M. Baylor. 1991. Myoplasmic calcium transients monitored with purpurate indicator dyes injected into intact frog skeletal muscle fibers. *Journal of General Physiology*. 97:245–270.
- Kovács, L., E. Ríos, and M. F. Schneider. 1983. Measurement and modification of free calcium transients in frog skeletal muscle fibres by a metallochromic indicator dye. *Journal of Physiology*. 343:161–196.
- Kress, M., H. E. Huxley, A. R. Faruqi, and J. Hendrix. 1986. Structural changes during activation of frog muscle studied by time-resolved X-ray diffraction. *Journal Molecular Biology*. 188:325–342.
- Lai, F. A., H. P. Erickson, E. Rousseau, Q.-Y. Liu, and G. Meissner. 1988. Purification and reconstitution of the calcium release channel from skeletal muscle. *Nature*. 331:315–319.

- MacLennan, D. H., and P. T. S. Wong. 1971. Isolation of a calcium-sequestering protein from sarcoplasmic reticulum. *Proceedings of the National Academy of Sciences, USA*. 68:1231–1235.
- Maylie, J., M. Irving, N. L. Sizto, and W. K. Chandler. 1987. Comparison of arsenazo III optical signals in intact and cut frog twitch fibers. *Journal of General Physiology*. 89:41–81.
- Melzer, W., E. Ríos, and M. F. Schneider. 1984. Time course of calcium release and removal in skeletal muscle fibers. *Biophysical Journal*. 45:637–641.
- Melzer, W., M. F. Schneider, B. J. Simon, and G. Szúcs. 1986. Intramembrane charge movement and calcium release in frog skeletal muscle. *Journal of Physiology*. 373:481–511.
- Neher, E. 1986. Concentration profiles of intracellular calcium in the presence of a diffusible chelator. In *Calcium Electrogenesis and Neuronal Functioning*. U. Heinemann, M. Klee, E. Neher, and W. Singer, editors. Springer-Verlag, Berlin. 80–96.
- Pape, P. C., D.-S. Jong, and W. K. Chandler. 1995. Calcium release and its voltage dependence in frog cut muscle fibers equilibrated with 20 mM EGTA. *Journal of General Physiology*. 106:259–336.
- Pape, P. C., D.-S. Jong, W. K. Chandler, and S. M. Baylor. 1993. Effect of fura-2 on action-potential stimulated calcium release in cut twitch fibers from frog muscle. *Journal of General Physiology*. 102:295–332.
- Pape, P. C., M. Konishi, and S. M. Baylor. 1992. Valinomycin and excitation-contraction coupling in skeletal muscle fibres of the frog. *Journal of Physiology*. 449:219–235.
- Pape, P. C., M. Konishi, S. Hollingworth, and S. M. Baylor. 1990. Perturbation of sarcoplasmic reticulum calcium release and phenol red absorbance transients by large concentrations of fura-2 injected into frog skeletal muscle fibers. *Journal of General Physiology*. 96:493–516.
- Pizarró, G., and E. Ríos. 1994. Simon's paradox. Local inactivation of Ca release in skeletal muscle. *Biophysical Journal*. 66:A339. (Abstr.)
- Prieto, H., P. Donoso, P. Rodriguez, and C. Hidalgo. 1994. Intraluminal calcium affects markedly calcium release rates in triads from rabbit but not from frog. *Biophysical Journal*. 66:A339. (Abstr.)
- Rakowski, R. F., P. M. Best, and M. R. James-Kracke. 1985. Voltage dependence of membrane charge movement and calcium release in frog skeletal muscle fibres. *Journal of Muscle Research and Cell Motility*. 6:403–433.
- Ríos, E., and G. Brum. 1987. Involvement of dihydropyridine receptors in excitation-contraction coupling in skeletal muscle. *Nature*. 325:717–720.
- Ríos, E., and G. Pizarró. 1988. Voltage sensors and calcium channels of excitation-contraction coupling. *News in Physiological Sciences*. 3:223–227.
- Schneider, M. F., and B. J. Simon. 1988. Inactivation of calcium release from the sarcoplasmic reticulum in frog skeletal muscle. *Journal of Physiology*. 405:727–745.
- Schneider, M. F., B. J. Simon, and G. Szúcs. 1987. Depletion of calcium from the sarcoplasmic reticulum during calcium release in frog skeletal muscle. *Journal of Physiology*. 392:167–192.
- Simon, B. J., and D. A. Hill. 1992. Charge movement and SR calcium release in frog skeletal muscle can be related by a Hodgkin-Huxley model with four gating particles. *Biophysical Journal*. 61:1109–1116.
- Simon, B. J., M. G. Klein, and M. F. Schneider. 1991. Calcium dependence of inactivation of calcium release from the sarcoplasmic reticulum in skeletal muscle fibers. *Journal of General Physiology*. 97:437–471.
- Simon, B. J., and M. F. Schneider. 1988. Time course of activation of calcium release from sarcoplasmic reticulum in skeletal muscle. *Biophysical Journal*. 54:1159–1163.
- Simon, B. J., M. F. Schneider, and G. Szúcs. 1985. Inactivation of sarcoplasmic reticulum calcium release in frog skeletal muscle is mediated by calcium. *Journal of General Physiology*. 86:36a. (Abstr.)
- Smith, J. S., R. Coronado, and G. Meissner. 1986. Single-channel measurements of the calcium release channel from skeletal muscle sarcoplasmic reticulum. *Journal of General Physiology*. 88:573–588.

- Smith, J. S., T. Imagawa, J. Ma, M. Fill, K. P. Campbell, and R. Coronado. 1988. Purified ryanodine receptor from rabbit skeletal muscle is the calcium-release channel of sarcoplasmic reticulum. *Journal of General Physiology*. 92:1–26.
- Somlyo, A. V., H. Shuman, and A. P. Somlyo. 1977. Elemental distribution in striated muscle and effects of hypertonicity: electron probe analysis of cryo sections. *Journal of Cell Biology*. 74:828–857.
- Tanabe, T., K. G. Beam, J. A. Powell, and S. Numa. 1988. Restoration of excitation-contraction coupling and slow calcium current in dysgenic muscle by dihydropyridine receptor complementary DNA. *Nature*. 336:134–139.
- Tinker, A., and A. J. Williams. 1992. Divalent cation conduction in the ryanodine receptor channel of sheep cardiac muscle sarcoplasmic reticulum. *Journal of General Physiology*. 100:479–493.
- Tinker, A., A. R. G. Lindsay, and A. J. Williams. 1992. A model for ionic conduction in the ryanodine receptor channel of sheep cardiac muscle sarcoplasmic reticulum. *Journal of General Physiology*. 100:495–517.
- Tinker, A., A. R. G. Lindsay, and A. J. Williams. 1993. Cation conduction in the calcium release channel of the cardiac sarcoplasmic reticulum under physiological and pathophysiological conditions. *Cardiovascular Research*. 27:1820–1825.